2020

DISSOLVED ORGANIC MATTER MOVEMENT ACROSS LAKE SUPERIOR'S TERRESTRIAL-STREAM-COASTAL INTERFACE

Karl M. Meingast
Michigan Technological University, kmmeinga@mtu.edu

DISSOLVED ORGANIC MATTER MOVEMENT ACROSS LAKE SUPERIOR'S TERRESTRIAL-STREAM-COASTAL INTERFACE

By

Karl M. Meingast

A DISSERTATION

Submitted in partial fulfillment of the requirements for the degree of

DOCTOR OF PHILOSOPHY

In Forest Science

MICHIGAN TECHNOLOGICAL UNIVERSITY

2020

This dissertation has been approved in partial fulfillment of the requirements for the Degree of DOCTOR OF PHILOSOPHY in Forest Science.

College of Forest Resources and Environmental Science

Dissertation Advisor:	*Dr. Evan Kane*
Committee Member:	*Dr. Amy Marcarelli*
Committee Member:	*Dr. Colleen Mouw*
Committee Member:	*Dr. Joseph Wagenbrenner*
College Dean:	*Dr. Andrew Storer*

Table of Contents

Preface

This dissertation includes three multi-authored manuscripts planned for publication. Included below are details regarding the status and author contributions for each chapte r:

Chapter 1 – *Climate, snowmelt dynamics and atmospheric deposition interact to control dissolved organic carbon export from a northern forest stream over 26 years,* this manuscript has been submitted and is *in review* with Environmental Research Letters. Robert Stottlemyer and Dave Toczydlowski designed the experiment and collected the data. Karl Meingast and Evan Kane conducted the analysis. Karl Meingast wrote the manuscript and created the figures. Ashley Coble and Amy Marcarelli provided editorial advice.

Chapter 2 – *Seasonal trends of DOM character in leachates, soils, and stream change with snowmelt timing,* this manuscript is planned for submission in the journal for Water Resources Research in the near future. Karl Meingast and Evan Kane conceived the study design. Karl Meingast collected the data. Karl Meingast analyzed the data. Karl Meingast made the figures and wrote the manuscript. Joseph Wagenbrenner and Amy Marcarelli provided editorial advice.

Chapter 3 – *Dissolved organic matter properties and remote sensing reflectance of river-sourced plumes in Lake Superior,* this manuscript is planned for submission in the Journal of Great Lakes Research in the near future. Karl Meingast conceived the study design and instrumentation setup. Colleen Mouw provided guidance on collection of data and assistance on processing of the data. Karl Meingast collected the data, analyzed the data, created the figures and wrote the manuscript. Evan Kane provided editorial advice.

Acknowledgements

The authors would like to thank Dr. Robert Stottlemyer for original study design and purveyance of long-term data in Chapter 1. All three chapters of this work were supported by the USDA-Funded McIntire-Stennis Program and with in-kind support from the USDA Forest Service, Northern Research Station. The NASA Earth and Space Science Fellowship supported Karl Meingast for all the Chapters. We thank Brice Grunert and Tim Veverica for assistance with chemometrics in Chapters 2 and 3. We thank Vince Beltrone for soil profile descriptions in Chapter 2. We appreciate discussions focused on DOM properties with Sarah Green, Amna Ijaz and Nastaran Khademimoshgenani, which improved this dissertation immensely. Karl Meingast would also like to thank his friends and family for their loving support through the completion of this dissertation. Finally, Karl Meingast would like to whole-heartedly thank Evan Kane for the advice and dedication to this project and Karl's scientific passions. It was an amazing opportunity to get to work with such a kind, thoughtful, passionate and dedicated advisor. It will be a great honor to professionally work together in the future.

Abstract

Dissolved organic matter (DOM) represents a carbon pool that can be easily translocated between ecosystems with the movement of water. This study examines the controls on DOM quantity and character delivered to Lake Superior primarily during the snowmelt period. We employed long-term stream dissolved organic carbon (DOC) data to determine quantity as well as absorption and fluorescence spectroscopy to analyze DOM structure. Our results indicate that an increasing trend in DOC concentrations, likely driven by decreases in acidity of precipitation, combined with slightly less annual runoff have resulted in relatively constant fluxes of DOM to Lake Superior. Additionally, our study displayed optical changes in DOM translocated from surface litter to deeper mineral soils that changed throughout the progression of snowmelt on different geomorphic aspects, but these changes did not reflect simultaneous pulses of snowmelt at the watershed scale. To aid in future monitoring of DOM translocated to Lake Superior via snowmelt, we developed a relationship between absorbance and dissolved organic carbon concentrations (DOC) for coastal Lake Superior and make recommendations for satellite retrievals of DOM absorbance as a proxy for DOC concentrations.

1 Climate, snowmelt dynamics and atmospheric deposition interact to control dissolved organic carbon export from a northern forest stream over 26 years

Karl M. Meingast [1]

Evan S. Kane[1, 2]

Ashley A. Coble[3]

Amy M. Marcarelli[4]

Dave Toczydlowski[4]

[1] Michigan Technological University; College of Forest Resources and Environmental Science; Houghton, MI

[2] U.S.D.A. Forest Service; Northern Research Station; Houghton, MI

[3] National Council for Air and Stream Improvement, Inc.; Corvallis, OR

[4] Michigan Technological University; Department of Biological Sciences; Houghton, MI

1.1 Abstract

Increasing concentrations of dissolved organic carbon (DOC) have been identified in many freshwater systems over the last three decades. Studies have generally nominated atmospheric deposition as the key driver of this trend, with changes in climatic factors also contributing. However, there is still much uncertainty concerning net effects of these drivers on DOC concentrations and export dynamics. Changes in climate and climate mediated snowfall dynamics in northern latitudes have not been widely considered as causal factors of changes

in long-term DOC trends, despite their disproportionate role in annual DOC export. We leveraged long-term datasets (1988-2013) from a first-order forested tributary of Lake Superior to understand causal factors of changes in DOC concentrations and exports from the watershed, by simultaneously evaluating atmospheric deposition, temperature, snowmelt timing, and runoff. We observed increases in DOC concentrations of approximately 0.14 mg C L^{-1} $year^{-1}$ (mean = 8.12 mg C L^{-1}) that were related with declines in sulfate deposition (0.03 mg SO_4 L^{-1} $year^{-1}$). Path analysis revealed that DOC exports were driven by runoff related to snowmelt, with peak snow water equivalences generally being lower and less variable in the 21st century, compared with the 1980s and 1990s. Mean temperatures were negatively related to maximum snow water equivalences (-0.71), and in turn had negative effects on DOC concentrations (-0.58), the timing of maximum discharge (-0.89) and DOC exports (indirect effect, -0.41). Based on these trends, any future changes in climate that lessen the dominance of snowmelt on annual runoff dynamics— including an earlier peak discharge— would decrease annual DOC export in snowmelt dominated systems. Together, these findings further illustrate complex interactions between climate and atmospheric deposition in carbon cycle processes, and highlight the importance of long-term monitoring efforts for understanding the consequences of a changing climate.

1.2 Introduction

Long-term studies of brown-water fed freshwater bodies have revealed increasing concentrations of dissolved organic carbon (DOC) over the last three decades across North America and Europe (Roulet and Moore 2006, Stottlemyer and Toczydlowski 2006, De Wit *et al* 2007, Monteith *et al* 2007a, Erlandsson *et al* 2008, Zhang *et al* 2010, Urban *et al* 2011, Couture *et al* 2012, De Wit *et al* 2016, Strock *et al* 2017). Mechanisms explaining increases in stream DOC concentrations have converged on changes in atmospheric deposition (De Wit *et al* 2007, Erlandsson *et al* 2008, Strock *et al* 2014), the timing and amounts of precipitation (Stottlemyer and Toczydlowski 2006, Erlandsson *et al* 2008, De Wit *et al* 2016), and responses to changing climate (Tiwari *et al* 2018). However, exactly how increases in DOC concentrations relate to DOC exports from watersheds are uncertain, as isolating factors controlling hydrologic connectivity within watersheds is difficult (Hood *et al* 2003, Couture *et al* 2012).

Winter snowpack is a dominant source of annual runoff in northern regions, and as such determines the dynamics of nutrient and DOC export (Buffam *et al* 2001). Therefore, changes in climate that alter the patterns of precipitation are likely to change the timing and amount of melt and runoff in snowmelt-dominated systems, potentially changing stream DOC concentrations and/or exports (Erlandsson *et al* 2008, Oni *et al* 2014). Shorter winters accompanied by lower snowmelt runoff peaks and slower spring snowmelt rates

are expected to be the largest effects of changing climate on snowmelt dynamics (Hayhoe *et al* 2010, Musselman *et al* 2017, Byun *et al* 2018). Given these predictions, total runoff is expected to decline as the relative amount of total precipitation contributed as snowfall declines. While there could be an increase in the frequency of autumn storms (e.g., Small *et al* 2006), it can also be expected that snowmelt will occur earlier with a longer snowmelt runoff hydrograph. Exactly how these factors are likely to correspond with changes in solute export from watersheds are uncertain.

Hydrologic flowpath variability has direct and indirect impacts on DOC export that may be countervailing under changing climate (Stottlemyer and Toczydlowski 2006). For example, if there is extensive and persistent snow water equivalent (SWE) contributing to a late onset of melt, this could lead to more DOC export through shallow carbon-rich soil flow paths, and higher variation in runoff and DOC export (e.g., Sebestyen *et al* 2008). Diminished SWE and early melt, which is increasingly likely in the future (Ågren *et al* 2010, Musselmen *et al* 2017; Byun *et al* 2018), should be coincident with less DOC export owing to reduced runoff. Moreover, a diminished or variable snowpack results in very different soil thermal gradient and decomposition environment, which also affects soil DOC concentrations (Li *et al* 2019). Given these complexities, changes in both DOC concentrations and the timing and amounts of runoff are likely to vary with peak SWE in ways that make understanding patterns of DOC export difficult.

Furthermore, it is unclear how potential changes in DOC concentrations in different flow paths could manifest as total DOC export, as disentangling the many factors governing hydrologic connectivity between soils and aquatic systems are also complex (Stottlemyer and Toczydlowski 1991, 2006).

Long-term changes in precipitation chemistry are also likely affecting DOC concentrations in streams. For example, sulfate (SO_4) deposition in precipitation increases the ionic strength in soils, which inhibits the release of organic acids (Krug and Frink 1983, Evans *et al* 2008). After amendments to air pollution legislation in the early 1990's - 2000's (e.g., U.S. Clean Air Act (1990); European Environment Agency, National Emission Ceilings Directive 81/EC (2001)), the rate of SO_4 deposition has declined (Strock *et al* 2014). The decline in SO_4 deposition and corresponding changes in soil ionic strength provides an explanation for the increased DOC concentrations observed in surface waters (Monteith *et al.* 2007a), but does not directly inform mechanisms controlling runoff and DOC export dynamics. Moreover, field studies observing interactive effects of SO_4 deposition and changes in runoff patterns over time are rare for snowmelt-dominated watersheds (De Wit *et al* 2007, Erlandsson *et al* 2008).

We examined the influence of snowmelt dynamics and climate on DOC concentrations and exports through analyses of long-term monitoring data for a small forested tributary of Lake Superior (Stottlemyer and Toczydlowski 2006). Because these factors are not easily isolated, long-term monitoring provides

useful insight into the dynamics of DOC concentrations and exports in response to climatic forcing and changes in atmospheric deposition. Specifically, we investigated changes in snowmelt runoff, temperatures, SO_4 deposition, and their interactive effects in explaining the variation in DOC concentrations and DOC exports over 26 years. We hypothesized that while peak snowpack runoff should primarily determine quantity of DOC exports, the timing of snowmelt would explain year-to-year variation in DOC export, with later peak melt events driving higher levels of DOC export. These analyses address our over-arching question: Given that long-term changes in SO_4 deposition have likely influenced DOC concentrations, do changes in snowmelt patterns explain additional variation in DOC concentrations in addition to DOC exports from snowmelt-dominated watersheds?

1.3 Methods

1.3.1 Study site

The Calumet watershed is a first-order tributary of Lake Superior in the Upper Peninsula of Michigan, USA (Latitude: 47.278, Longitude: -88.515), previously described in detail by Stottlemyer and Toczydlowski (2006). Briefly, the watershed is 176-ha, has uniform slope (5%), moderate topographic relief and is vegetated by mixed northern hardwood forest. Soils are Typic Haplorthods with an ortstein layer at 1.5 – 2.0 m depth (Stottlemyer and Toczydlowski 1991).

The climate is modified by Lake Superior, which moderates autumn and winter temperature extremes (Stottlemyer and Toczydlowski 2006). The National Atmospheric Deposition Program (NADP) site (MI99) is located 16 km south of the watershed, and received a mean of 803 mm in annual precipitation over the study period (Supplemental Figure; Figure S1). The annual hydrograph is dominated by snowmelt and can be highly variable in timing and duration. The transitional spring climate has a large impact on the timing and duration of the spring snowmelt hydrograph (Figure 1).

1.3.2 Field procedures

Snow cores were measured weekly typically from mid-December to mid-April across four transects spanning the elevation gradient at Calumet, 1988-2013 (Stottlemyer and Toczydlowski 1991). The transects consisted of five sampling points and were measured weekly using a Federal sampler for snow moisture content (Stottlemyer and Toczydlowski 2006). These transects were averaged for a watershed SWE estimate. Continuous stream discharge was monitored using a 30-cm wide Parshall flume equipped with a Li-Cor datalogger and Stevens pressure transducer. Continuous data were integrated by day to calculate a daily measurement of runoff. Stream water samples were collected approximately weekly except during snowmelt, when samples were collected multiple times per week to capture the leading and trailing edges of the hydrograph. Water samples were collected in amber polyethylene 500-ml bottles

and frozen for later analysis. Precipitation chemical composition data was acquired from the NADP monitoring site MI99 in Chassell, MI and was used to obtain monthly averages of SO_4 deposition (wet deposition) for the study period (1988-2013). Daily temperature data was collected from the National Oceanic and Atmospheric Administration (NOAA) station 3908 Houghton-Hancock County Airport 8 km south of the watershed.

1.3.3 Laboratory analysis

Water samples were immediately brought to Michigan Technological University for analysis. DOC sample analysis is described in detail by (Stottlemyer and Toczydlowski 2006). Briefly, for the period (1988-1997) DOC was determined on filtered samples (0.45 μm) using a Dohrmann 180 (Teledyne-Tekmar-Dohrmann, Mason, Ohio) carbon analyzer. Post 1997, DOC concentrations were determined using a Shimadzu TOC-5000A analyzer (Shimadzu Scientific Instruments, Columbia, Maryland). Laboratory quality assurance procedures were previously described in detail (Stottlemyer and Toczydlowski 2006), and included analyses of split samples run as part of NADP, the Environmental Protection Agency's National Acid Precipitation Assessment Program (NAPAP) and continuous participation in the U.S. Geological Survey laboratory round robin program.

1.3.4 Data analysis

1.3.4.1 Snowmelt descriptors

Maximum SWE was calculated for each year. Maximum discharge date was defined as the date of the spring hydrograph peak. Traditionally, spring melt onset for river and stream discharge has been defined as the center of volume date (Hodgkins *et al* 2003). However, center of volume date does not necessarily reflect the onset of increased hydrologic connectivity with soils and snowpack. Therefore, we developed a metric based on the leading edge of the stream snowmelt hydrograph to identify the critical timing of the initial onset of spring (see for example, Contosta *et al* 2017). For this study, melt initiation was defined as the first day when a four-fold increase in stream discharge relative to winter baseflow was observed and sustained for a minimum of four consecutive days. Early and late melts were defined by the melt initiation date for a given year in relation to the median melt initiation date for the study period. To further characterize the duration of the spring freshet, we calculated the duration between melt initiation and peak runoff, hereafter referred to as steep time (days).

1.3.4.2 Statistical analysis

Because sampling was not conducted at a constant frequency, linear interpolation with respect to time was used to estimate DOC concentrations on a daily timestep, matching the temporal resolution of daily discharge

measurements. One DOC collection reflected an ephemeral pulse of rain after the hydrograph peak, yielding a low value (0.08 mg C L^{-1}) that was not used for interpolation (see supplemental online material).

Linear regression analysis was used to test for significant trends in annual hydrologic and snowmelt variables for the time period (1988-2013; n = 26). Trends were reported if significant at $p < 0.05$. Bartlett tests were performed at three-year intervals on annual time series data to test for non-constant variance across years (Bartlett, 1937). These trend analyses were conducted in R (version 3.3.2; R Core Team, 2017). In our 26-year dataset, we examined broader changes in atmospheric SO_4 deposition, water year, mean annual air temperature, maximum winter SWE, and annual runoff, and tested for interactive effects on mean annual DOC concentrations and exports. We used a path analysis approach (Wright, 1934) on annual descriptors, which enabled analysis of both direct and indirect effects on DOC concentrations and exports. We used the Calis procedure (LINEQS; SAS version 9.4, SAS Institute, Cary, North Carolina, USA) with the date of maximum stream discharge, maximum SWE, mean air temperature, and mean precipitation SO_4 concentration as exogenous variables with paths to mean stream DOC concentration and mean DOC export; DOC concentration also had a path to DOC export. These exogenous variables were chosen to appropriately constrain the model without statistical redundancies (i.e., autocorrelation among variables, such as peak SWE and runoff). Error

terms (STD statement) were estimated for DOC concentration and DOC export. The model was evaluated through examination of Standardized Root Mean Square Residual (SRMR) and the Bentler Comparative Fit Index (CFI; model accepted at < 0.08 and > 0.99, respectively; Hu and Bentler 1999). We report results from the covariance structure analysis (maximum likelihood estimation) for standardized direct and indirect effects (significant at $p < 0.05$).

1.4 Results

1.4.1 Changes in hydroclimate

Variation in the onset of melt, and hence the duration of winter, as well as snowpack depth have changed over time. The occurrences of winters associated with high maximum SWE and extended snowmelt through the spring have declined over the study period (Bartlett test; $p = 0.034$; $n = 26$ years) (Figure 2a). Annual cumulative runoff exhibited a marginally significant downward trend of 2.4 mm Y^{-1} (S.E. = 1.2 mm Y^{-1}) ($R^2 = 0.11$, $p = 0.05$; Figure 2b). Steep time also showed decreasing variation through time, indicating spring climate is becoming more homogenous with less frequent extended snowmelt periods (Bartlett test; $p = 0.023$; $n = 26$ years) (Figure 2c). There were no trends in temperature within the range of records reflected in this study (1988-2013). Temperature records extend beyond the solute records in this study (1948 – 2018), and there has been a long-term increase in air temperatures observed in August and September of 0.026 °C Y^{-1} (S.E. = 0.010 °C Y^{-1}) and 0.034 °C Y^{-1} (S.E. = 0.009

°C Y^{-1}), respectively (Figure S2). However, annual mean temperature did not show a significant warming trend (mean of 4.5 °C).

1.4.2 DOC concentrations and export

Stream DOC concentration ranged from 2.61 mg C L^{-1} to 20.00 mg C L^{-1} (mean = 8.12 mg C L^{-1} over the course of the study). Mean annual DOC concentrations increased significantly by 0.14 mg C L^{-1} Y^{-1} (S.E. = 0.03 C L^{-1} Y^{-1}) (Figure 2d). SO_4 concentrations in precipitation have been decreasing by approximately 0.026 mg L^{-1} Y^{-1} (S.E. = 0.003 mg L^{-1} Y^{-1}) in Northern Michigan (1988 -2013; National Atmospheric Deposition Program; MI99; Figure S3). Path analysis indicated that SO_4 concentration had a direct negative effect (-0.57, $p < 0.0001$) on DOC concentrations in the stream (Figure 3). The path analysis also highlighted the negative effect of mean temperature on DOC concentrations (-0.58, $p = 0.016$), owing to the strong direct negative effects of mean temperature on maximum SWE (-0.71, $p < 0.001$) and in turn of maximum SWE on DOC concentrations (-0.77, $p = 0.001$).

Annual runoff showed a significant correlation with maximum SWE ($R^2 = 0.57$, $p < 0.0001$; Figure 4a). Annual runoff also correlated with annual DOC export ($R^2 = 0.51$, $p < 0.0001$; Figure 4b). There was a correlation between maximum SWE and annual DOC export ($R^2 = 0.18$, $p = 0.02$) and maximum SWE had a positive direct effect on DOC export in path analysis (Figure 3). Because maximum SWE was strongly negatively related to mean temperature,

temperature also had a negative indirect effect on DOC export in path analysis (-0.41, p = 0.002; indirect path data not shown). Melt onset date and peak discharge date correlated strongly with annual DOC export (Figure 5), and as such later maximum discharge corresponded to higher DOC exports (significant positive direct effect, 0.24, p = 0.038; Figure 3). In addition, maximum SWE was also positively related to the timing of maximum discharge in path analysis (0.82, p < 0.001). Steep time, or the duration of melt, was not significantly related to annual mean stream DOC concentration or export (p = 0.5).

1.5 Discussion

1.5.1 DOC concentration

Path analysis indicated that maximum SWE had a negative influence on DOC concentrations, likely through dilution effects (Figure 3). However, the strength of this effect would be diminished if trends in maximum SWE continue to decline and if warming trends extend into the spring season. Mean temperatures had a negative effect on DOC concentrations in the path analysis conducted in this study. Prior research has observed an increase in DOC release in soils that experience freezing conditions, suggesting that the integrated effect of air temperature and winter snow cover duration drives soil frost formation and subsequently stream DOC concentrations (Haei *et al* 2010). The mechanism by which soil freezing increases DOC concentrations is likely a combination of increased solutes from root and microbial mortality (cell lysis) and solute

concentration by freezing (Biederbeck and Campbell 1971, Fitzhugh *et al* 2001, Agren *et al* 2012). In addition to these mechanisms, we highlight here that soils in this study region typically do not freeze in the winter, because the depth and persistence of the snowpack; this effectively disconnects winter soil and air temperatures. It is possible that warmer fall temperatures (cf. Figure S2) could attenuate snowpack formation, permitting freezing conditions in soils (Groffman *et al* 2001) and thus promoting the release of DOC (Fitzhugh *et al* 2001, Haei *et al* 2012).

Stream DOC concentrations have been steadily increasing over the last three decades, while atmospheric SO_4 concentrations have declined. The steady decline in SO_4 deposition offers a parsimonious explanation for the increase in observed DOC concentrations. In addition, we highlight here that runoff appears to affect DOC concentrations and water delivery that drives export. Future work is needed to tease apart the complex role climate plays in mediating runoff, particularly in snowmelt dominated watersheds. These findings are in line with previous studies that have identified atmospheric deposition as the principal driver of increased DOC concentrations in surface waters, while highlighting the important influences of climate factors with strong seasonal effects on carbon export dynamics (see Clark *et al* 2010, and references therein).

1.5.2 DOC export

Winter snowpack has the largest direct effect on DOC export through runoff (Figure 4). Additionally, snowmelt timing shows a positive correlation with annual DOC export for the watershed, which is also influenced by snow water equivalences (Figure 3). These results indicate that the amount of water in the snow is more significant than the timing of snowmelt in controlling DOC export, and temperature appears to have a greater effect on timing than snow water equivalence (Figure 3), which could alter the relative magnitudes of these effects in the future. The decline in runoff over time (Figure 2b) along with the direct and indirect effects of snowmelt and temperature on export (Figure 3) offer countervailing effects which result in no time trend for DOC export. Other studies of temperate zone streams have also identified an increase in stream DOC concentrations with no associated increase in export (Urban *et al* 2011, Coble *et al* 2018, O'Driscoll *et al* 2018). Our analysis suggests that slight changes in runoff combined with indirect controls of temperature and snowmelt can offset effects of increased DOC concentrations and attenuate DOC exports. However, this is further complicated by the co-occurrence of slow-melt and low snowpack years (denoted by subscript letters (b) and (d) in Figure 1; Table 1), which add considerable variation to interannual DOC exports (Figure 5).

The large proportion of seasonal precipitation falling as snow is a distinctive characteristic of watersheds in the northern Great Lakes region like

the Calumet watershed, as it consistently provides a baseline minimum amount of water in spring runoff capable of flushing a minimum amount of DOC each year. While variation in snowpack in the Calumet watershed among years was quite high, the record shows there was always at least approximately 180 mm of water in peak snowpack (Figure 2a). As such, runoff contributions from rainfall would have to be very large events - around 180 mm of precipitation in a given storm - to significantly alter the shape of the snowmelt-dominated hydrograph (e.g., Figure 1). While larger and more variable storms are expected to occur more frequently in the Great Lakes region (Kossin *et al* 2017), the spring freshet is likely to remain the largest pulse of DOC export from watersheds in this region. Late fall runoff was generally the second largest pulse of DOC from the watershed. Late summer baseflow has been related to maximum SWE in mountainous regions (Godsey *et al* 2014; Barnhart et al. 2016). In this study, July and August runoff showed significant linear trends with both maximum SWE (R^2 = 0.65; $p < 0.0001$ and R^2 = 0.38; p = 0.0003 respectively; Figure S4; Figure S5) and melt initiation (R^2 = 0.64; $p < 0.0001$ and R^2 = 0.37; p =0.0004 respectively; Figure S4; Figure S5). Although speculative, this suggests that snowmelt recharge is significant for late summer baseflow conditions and subsequent DOC export. This highlights the importance of winter snowpack in these regions on the annual hydrograph and subsequent DOC exports.

1.5.3 A changing hydrograph

Given climate change predictions for areas with high snowfall (e.g., Musselman *et al* 2017), we expect changes in the hydrographs of snowmelt-dominated tributaries, with consequences for solute export (cf. Marcarelli *et al* 2019). Most notably, these predictions indicate earlier and slower snowmelt to prolong the hydrograph with an earlier melt onset. Although this 26-year study period contains more years in the late- than early-season melt scenario (15 and 11 years, respectively; Table 1), our results indicate that both earlier and slower snowmelt may lead to decreased DOC exports. Exactly how climate-induced changes in the spring hydrograph affect DOC exports will depend on the persistence of increasing DOC concentrations, snowmelt dynamics and temperature. While trends to date are best represented as linear processes, we stress here that the increasing DOC concentrations and declining peak SWE may exhibit non-linear or threshold responses in the future. For example, runoff cannot continue to decline at the same rate indefinitely, and the increasing DOC concentrations should reach a new stable state over time (Monteith *et al* 2007b). As such, long-term monitoring efforts are invaluable for detecting novel patterns of DOC export.

1.6 References

Ågren, A., Haei, M., Köhler, S. J., Bishop, K., & Laudon, H. (2010). Regulation of stream water dissolved organic carbon (DOC) concentrations during snowmelt; the role of discharge, winter climate and memory effects. *Biogeosciences*, *7*(9), 2901-2913.

Barnhart, T. B., Molotch, N. P., Livneh, B., Harpold, A. A., Knowles, J. F., & Schneider, D. (2016). Snowmelt rate dictates streamflow. *Geophysical Research Letters*, *43*(15), 8006-8016.

Bartlett, M. S. (1937). Properties of sufficiency and statistical tests. *Proceedings of the Royal Society of London. Series A-Mathematical and Physical Sciences*, *160*(901), 268-282.

Biederbeck, V. O., & Campbell, C. A. (1971). Influence of simulated fall and spring conditions on the soil system. I. Effect on soil microflora. *Soil Science Society of America Journal*, *35*(3), 474-479.

Buffam, I., Galloway, J. N., Blum, L. K., & McGlathery, K. J. (2001). A stormflow/baseflow comparison of dissolved organic matter concentrations and bioavailability in an Appalachian stream. *Biogeochemistry*, *53*(3), 269-306.

Byun, K., Chiu, C.M., & Hamlet, A.F. (2018). Effects of 21st century climate change on seasonal flow regimes and hydrologic extremes over the Midwest and Great Lakes region of the US. *Science of The Total Environment*, 650, 1261-1277.

Clark, J.M., Bottrell, S.H., Evans, C.D., Monteith, D.T., Bartlett, R., Rose, R., Newton, R.J. & Chapman, P.J., (2010). The importance of the relationship between scale and process in understanding long-term DOC dynamics. *Science of the total environment*, *408*(13), pp.2768-2775.

Coble, A. A., Wymore, A. S., Shattuck, M. D., Potter, J. D., & McDowell, W. H. (2018). Multiyear Trends in Solute Concentrations and Fluxes from a Suburban Watershed: Evaluating Effects of 100‐Year Flood Events. *Journal of Geophysical Research: Biogeosciences*, *123*(9), 3072-3087.

Contosta, A.R., Adolph, A., Burchsted, D., Burakowski, E., Green, M., Guerra, D., Albert, M., Dibb, J., Martin, M., McDowell, W.H. & Routhier, M., (2017). A longer vernal window: the role of winter coldness and snowpack in driving spring transitions and lags. *Global change biology*, *23*(4), pp.1610-1625.

Couture, S., Houle, D., & Gagnon, C. (2012). Increases of dissolved organic carbon in temperate and boreal lakes in Quebec, Canada. *Environmental Science and Pollution Research*, *19*(2), 361-371.

De Wit, H. A., Mulder, J., Hindar, A., & Hole, L. (2007). Long-term increase in dissolved organic carbon in streamwaters in Norway is response to reduced acid deposition. *Environmental Science & Technology*, *41*(22), 7706-7713.

de Wit, H.A., Valinia, S., Weyhenmeyer, G.A., Futter, M.N., Kortelainen, P., Austnes, K., Hessen, D.O., Räike, A., Laudon, H. & Vuorenmaa, J., (2016). Current browning of surface waters will be

further promoted by wetter climate. *Environmental Science & Technology Letters*, *3*(12), pp.430-435.

Erlandsson, M., Buffam, I., Fölster, J., Laudon, H., Temnerud, J., Weyhenmeyer, G. A., & Bishop, K. (2008). Thirty-five years of synchrony in the organic matter concentrations of Swedish rivers explained by variation in flow and sulphate. *Global Change Biology*, *14*(5), 1191-1198.

Evans, C. D., Monteith, D. T., Reynolds, B., & Clark, J. M. (2008). Buffering of recovery from acidification by organic acids. *Science of the Total Environment*, *404*(2-3), 316-325.

Fitzhugh, R. D., Driscoll, C. T., Groffman, P. M., Tierney, G. L., Fahey, T. J., Hardy, J. P. (2001). Effects of soil freezing disturbance on soil solution nitrogen, phosphorus, and carbon chemistry in a northern hardwood ecosystem. *Biogeochemistry*, 56, 215-238.

Godsey, S. E., Kirchner, J. W., & Tague, C. L. (2014). Effects of changes in winter snowpacks on summer low flows: case studies in the Sierra Nevada, California, USA. *Hydrological Processes*, *28*(19), 5048-5064.

Groffman, P. M., Driscoll, C. T., Fahey, T. J., Hardy, J.P., Fitzhugh, R.D., Tierney, G. L. (2001). Colder soils in a warmer world: a snow manipulation study in a northern hardwood forest ecosystem. *Biogeochemistry*, 56, 135–150.

Haei, M., Öquist, M.G., Buffam, I., Ågren, A., Blomkvist, P., Bishop, K., Ottosson Löfvenius, M. & Laudon, H. (2010). Cold winter soils enhance dissolved organic carbon concentrations in soil and stream water. *Geophysical Research Letters*, *37*(8).

Haei, M., Öquist, M.G., Ilstedt, U., Laudon, H. (2012). The influence of soil frost on the quality of dissolved organic carbon in a boreal forest soil: combining field and laboratory experiments. *Biogeochemistry*, 107, 95-106.

Hayhoe, K., VanDorn, J., Croley II, T., Schlegal, N., & Wuebbles, D. (2010). Regional climate change projections for Chicago and the US Great Lakes. *Journal of Great Lakes Research*, *36*, 7-21.

Hodgkins, G.A., Dudley, R.W. and Huntington, T.G. (2003). Changes in the timing of high river flows in New England over the 20th century. *Journal of Hydrology*, *278*(1-4), pp.244-252.

Hood, E., McKnight, D.M. and Williams, M.W. (2003). Sources and chemical character of dissolved organic carbon across an alpine/subalpine ecotone, Green Lakes Valley, Colorado Front Range, United States. *Water Resources Research*, *39*(7).

Hu, L. T., & Bentler, P. M. (1999). Cutoff criteria for fit indexes in covariance structure analysis: Conventional criteria versus new alternatives. *Structural equation modeling: a multidisciplinary journal*, *6*(1), 1-55.

Kossin, J.P., T. Hall, T. Knutson, K.E. Kunkel, R.J. Trapp, D.E. Waliser, and M.F. Wehner, (2017): Extreme storms. In: Climate Science Special Report: Fourth National Climate Assessment, Volume I [Wuebbles, D.J., D.W. Fahey, K.A. Hibbard, D.J. Dokken, B.C. Stewart, and T.K. Maycock (eds.)]. U.S. Global Change Research Program, Washington, DC, USA, pp. 257-276, doi: 10.7930/J07S7KXX.

Krug, E. C., & Frink, C. R. (1983). Acid rain on acid soil: a new perspective. *Science*, *221*(4610), 520-525.

Li, M., Wang, J., Guo, D., Yang, R., Fu, H. (2019). Effect of land management practices on the concentration of dissolved organic matter in soil: A meta-analysis. *Geoderma*, 344, 74-81.

Marcarelli, A.M., Coble, A.A., Meingast, K.M., Kane, E.S., Brooks, C.N., Buffam, I., Green, S.A., Huckins, C.J., Toczydlowski, D. & Stottlemyer, R., (2019). Of small streams and Great Lakes: integrating tributaries to understand the ecology and biogeochemistry of Lake Superior. *JAWRA Journal of the American Water Resources Association*, *55*(2), pp.442-458.

Monteith, D.T., Stoddard, J.L., Evans, C.D., De Wit, H.A., Forsius, M., Høgåsen, T., Wilander, A., Skjelkvåle, B.L., Jeffries, D.S., Vuorenmaa, J. & Keller, B., (2007a). Dissolved organic carbon trends resulting from changes in atmospheric deposition chemistry. *Nature*, *450*(7169), pp.537-540.

Monteith D.T., Stoddard J.L., Evans C.D., de Wit H.A., Forsius M., Hogasen T., Jeffries D.S., Kopacek J., Skjelkvale B.L., Vesely J., Vuorenmaa J., & Wilander A. (2007b). Increases in DOC in remote lakes and rivers: a signal of climate change or return to pre-acidification conditions? In: "Trends in surface water chemistry and biota; The importance of confounding factors, edited by: (de Wit H, Skjelkvåle BL eds). Norwegian Institute for Water Research, Oslo. ICP Waters Report 87/2007: 39-49.

Musselman, K.N., Clark, M.P., Liu, C., Ikeda, K. & Rasmussen, R. (2017). Slower snowmelt in a warmer world. *Nature Climate Change*, *7*(3), p.214.

O'Driscoll, C., Ledesma, J.L., Coll, J., Murnane, J.G., Nolan, P., Mockler, E.M., Futter, M.N. & Xiao, L.W., (2018). Minimal climate change impacts on natural organic matter forecasted for a potable water supply in Ireland. *Science of the total environment*, *630*, pp.869-877..

Oni, S., Futter, M., Ledesma, J., Teutschbein, C., Buttle, J., & Laudon, H. (2016). Using dry and wet year hydroclimatic extremes to guide future hydrologic projections. *Hydrology and Earth System Sciences*, *20*(7), 2811-2825.

R Core Team (2017). R: A language and environment for statistical computing. R Foundation for Statistical Computing, Vienna, Austria. URL https://www.R-project.org/.

Roulet, N. and Moore, T.R. (2006). Environmental chemistry: browning the waters. *Nature*, *444*(7117), p.283.

Sebestyen, S. D., Boyer, E. W., Shanley, J. B., Kendall, C., Doctor, D. H., Aiken, G. R., & Ohte, N. (2008). Sources, transformations, and hydrological processes that control stream nitrate and dissolved organic matter concentrations during snowmelt in an upland forest. Water Resources Research, 44, W12410.

Small, D., Islam, S., & Vogel, R., (2006). Trends in precipitation and streamflow in the eastern U.S.: paradox or perception? Geophysical Research Letters 33, L03403

Stottlemyer, R. and Toczydlowski, D., (1991). Stream chemistry and hydrologic pathways during snowmelt in a small watershed adjacent Lake Superior. *Biogeochemistry*, 13, 177-197.

Stottlemyer, R. and Toczydlowski, D. (2006). Effect of reduced winter precipitation and increased temperature on watershed solute flux, 1988–2002, Northern Michigan. *Biogeochemistry*, *77*(3), pp.409-440.

Strock, K.E., Nelson, S.J., Kahl, J.S., Saros, J.E. & McDowell, W.H., (2014). Decadal trends reveal recent acceleration in the rate of recovery from acidification in the northeastern US. *Environmental science & technology*, *48*(9), pp.4681-4689.

Strock, K.E., Theodore, N., Gawley, W.G., Ellsworth, A.C. & Saros, J.E. (2017). Increasing dissolved organic carbon concentrations in northern boreal lakes: Implications for lake water transparency and thermal structure. *Journal of Geophysical Research: Biogeosciences*, *122*(5), pp.1022-1035.

Tiwari, T., Sponseller, R. A., & Laudon, H. (2018). Extreme climate effects on dissolved organic carbon concentrations during snowmelt. *Journal of Geophysical Research: Biogeosciences*, *123*(4), 1277-1288.

Urban, N., Verry, E. S., Eisenreich, S., Grigal, D. F., & Sebestyen, S. D. (2011). Element cycling in upland/peatland watersheds. *Peatland Biogeochemistry and Watershed Hydrology at the Marcell Experimental Forest*, 213-241.

Wright, S. (1934). The method of path coefficients. *The annals of mathematical statistics*, *5*(3), 161-215.

Zhang, J., Hudson, J., Neal, R., Sereda, J., Clair, T., Turner, M., Jeffries, D., Dillon, P., Molot, L., Somers, K. & Hesslein, R. (2010). Long-term patterns of dissolved organic carbon in lakes across eastern Canada: Evidence of a pronounced climate effect. *Limnology and Oceanography*, *55*(1), pp.30-42.

1.7 Tables and Figures

Table 1: The 26 snowmelt hydrographs from this study, binned by melt timing and peak SWE. There has been large variation in seasonal snowpack and melt dynamics over the

last 26 years, with a general trend of high SWE with late melts and low SWE associated with early melts.

Melt timing	Peak SWE (# in last 26 years)	Likely future change	Likely DOC export
Early	High (1 year)	(?)	Variable. Fast has punctuated export whereas slow has stormflow influences
	Low (10 years)	(+)	
Late	High (10 years)	(-)	Generally high
	Low (5 years)	(?)	Variable

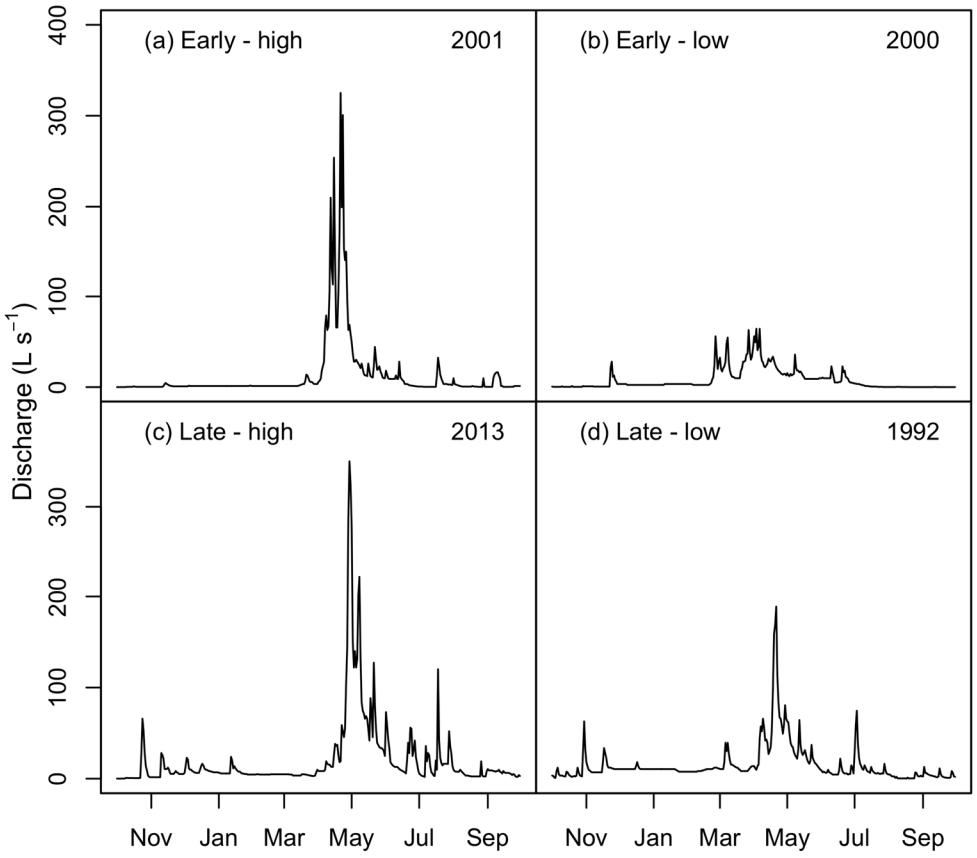

Figure 1: Four representative hydrographs of the stream at Calumet. (a) Early melt with high maximum SWE, (b) early melt with low maximum SWE, (c) late melt with high maximum SWE and (d) late melt with low maximum SWE. These four hydrographs correspond with the four melt scenarios proposed in Table 1

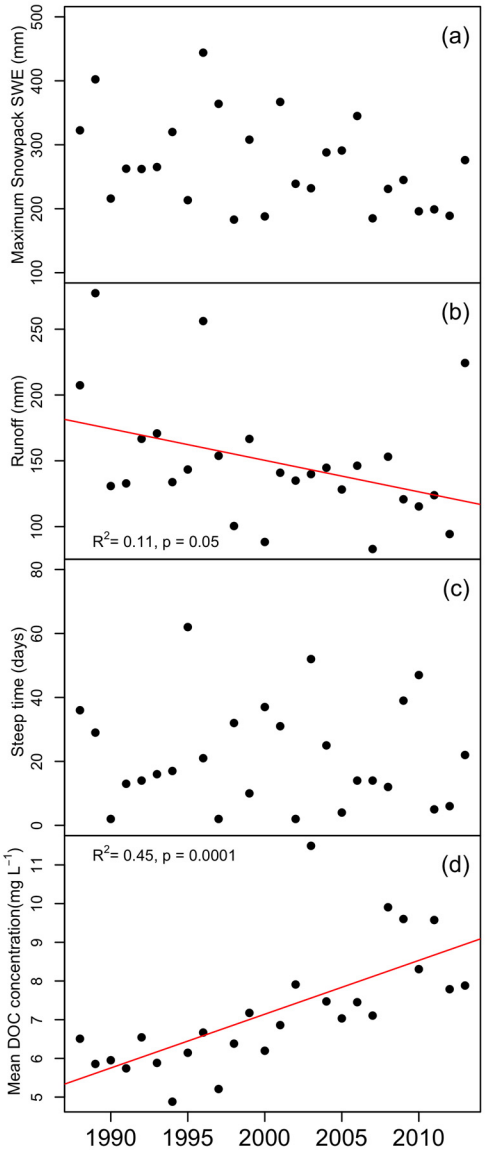

Figure 2: (a) Variation in snowpack maximum SWE has declined over the study period (Bartlett test; p = 0.034; n = 26 years). (b) There has been a marginal decline in annual runoff at Calumet Watershed over the last three decades. (c) Variation in spring melt duration (steep time) has declined over the study period (Bartlett test; p = 0.023). (d) DOC concentrations have been increasing at Calumet when plotted continuously and as yearly means (slope = 0.14 mg C L^{-1} Y^{-1}).

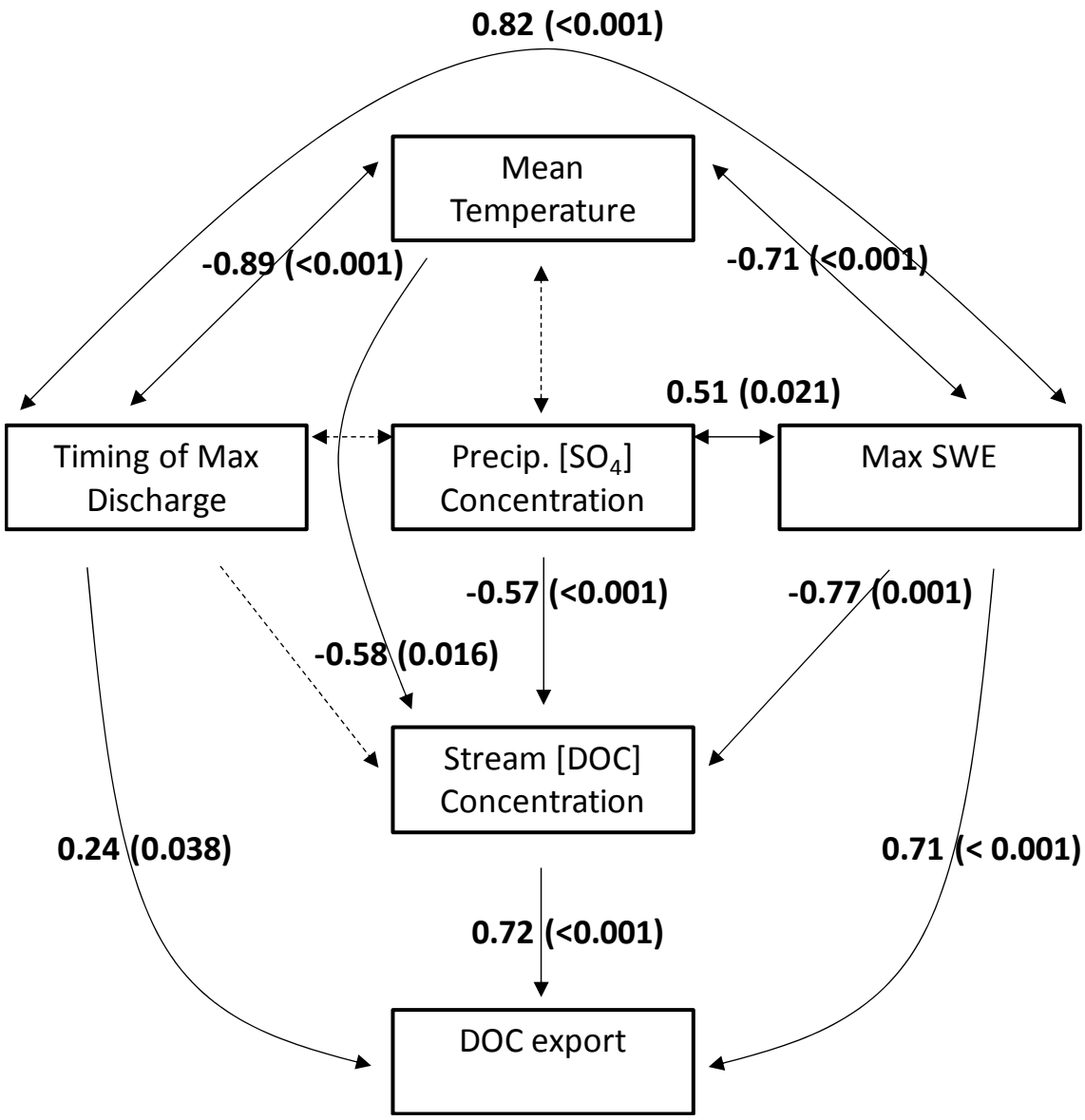

Figure 3: A path analysis used to test the effects of snowmelt dynamics, climate and atmospheric deposition on DOC concentrations and export (depicted here are direct effects). Bold text indicates significant effects (p value in parentheses; dashed lines are non-significant paths). Model Standardized Root Mean Square Residual (SRMR) = 0.004; Bentler Comparative Fit Index (CFI) = 0.994.

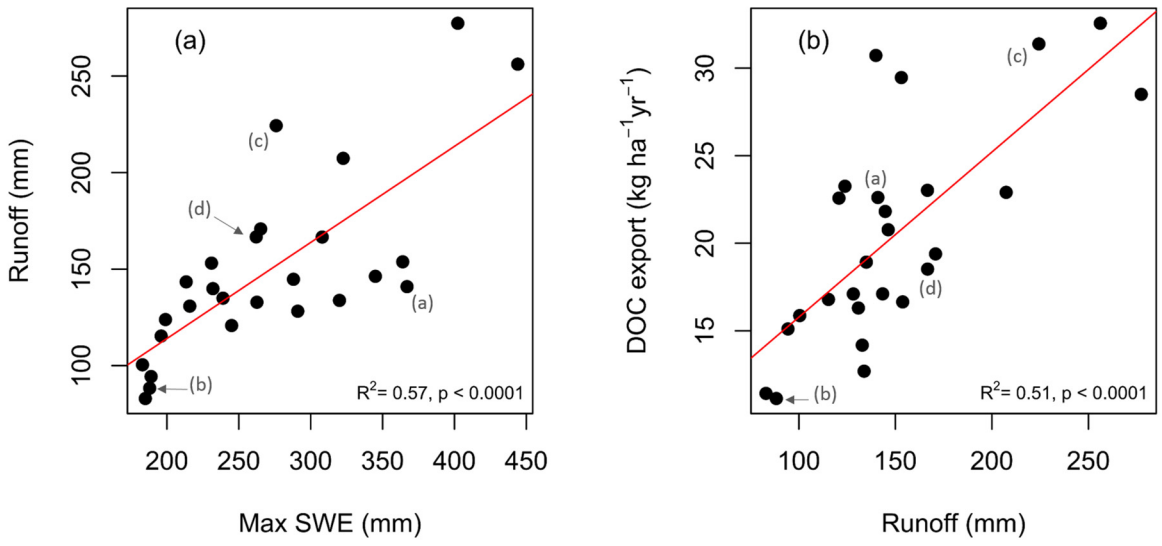

Figure 4: (a) Annual runoff (by water year) has been decreasing at the Calumet Watershed, which is correlated with changes in maximum SWE. (b) Runoff in turn is a major determinant of annual C export from this watershed. Grey letters correspond to representative water years in Figure 1.

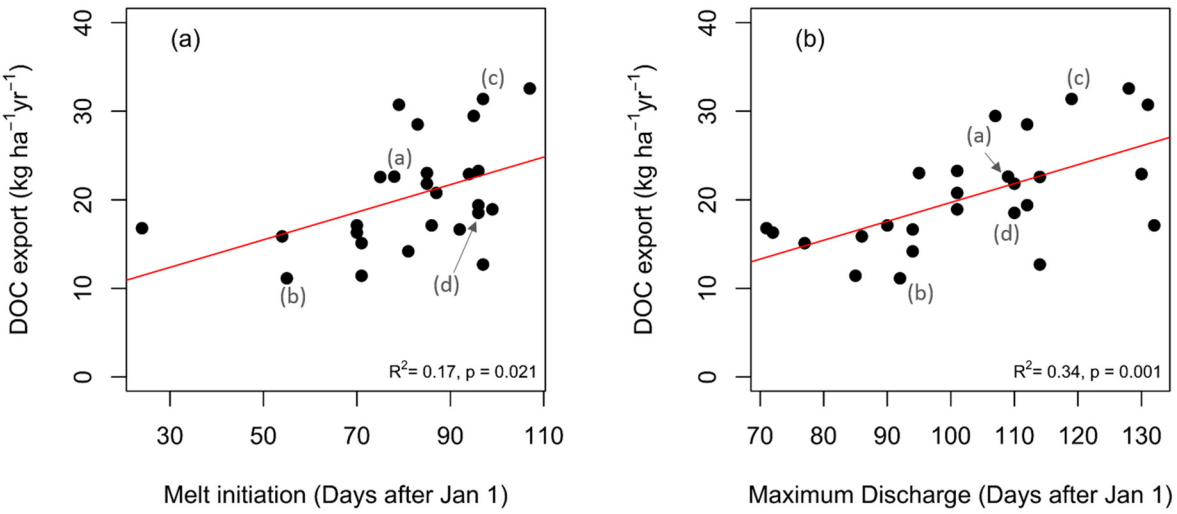

Figure 5: (a) Later onset of melt, a scenario which is predicted to occur less often in the future, has correlated with a greater export of carbon from Calumet Watershed. (b) The timing of maximum discharge is also correlated with DOC export, with later peak discharge resulting in greater carbon export (cf. Figure 3). Grey letters correspond to representative water years in Figure 1.

1.8 Supplemental material

Supplementary Information: Meingast et al., The importance of snowmelt dynamics on dissolved organic carbon export from a northern forest tributary over 26 years

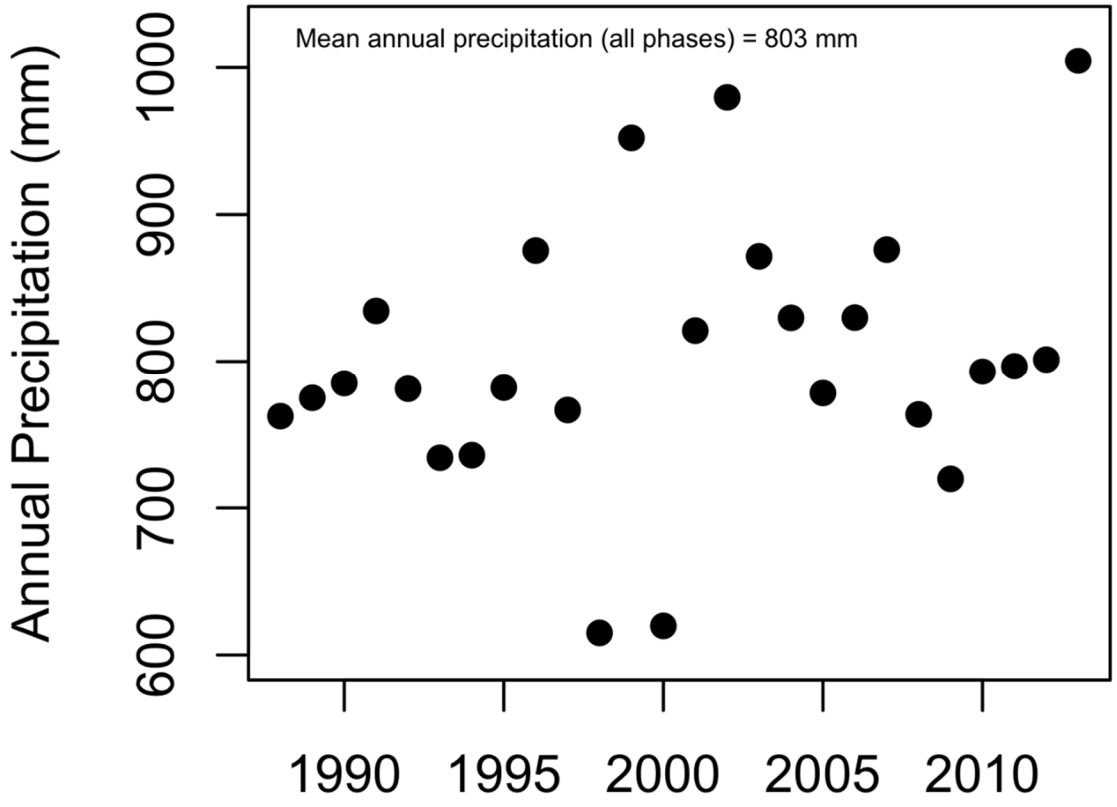

Figure S1: Cumulative annual precipitation at the National Atmospheric Deposition Program (NADP) site MI99 located 16 km south of the watershed from 1988 - 2013.

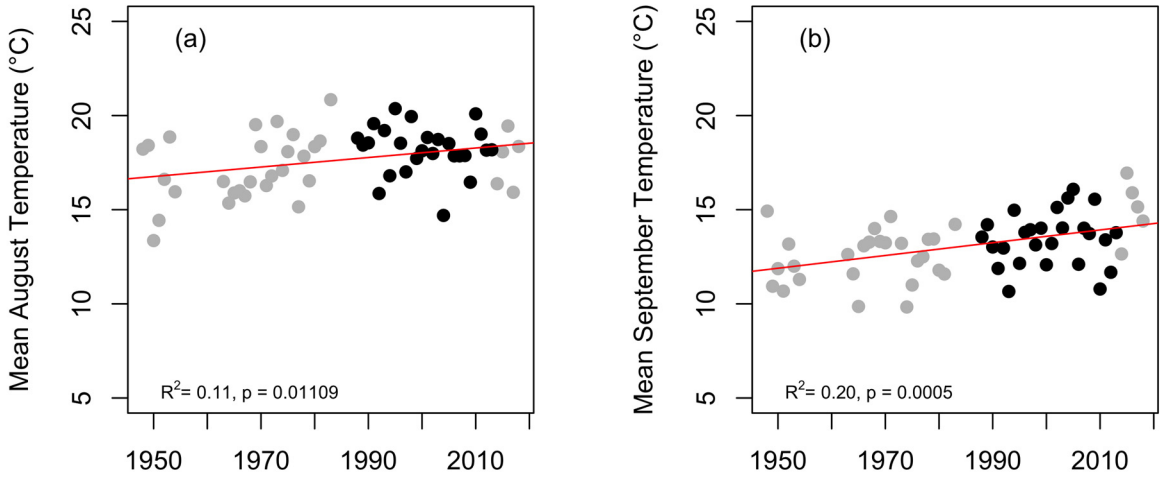

Figure S2: Mean August (a) and September (b) air temperatures show increasing trends from the Houghton County Airport 8 km south of the watershed (1948 – 2018). No other months displayed significant trends. Black points indicate years from this study period, however relationships were calculated for the entire record. Relationships limited to this study period were not significant.

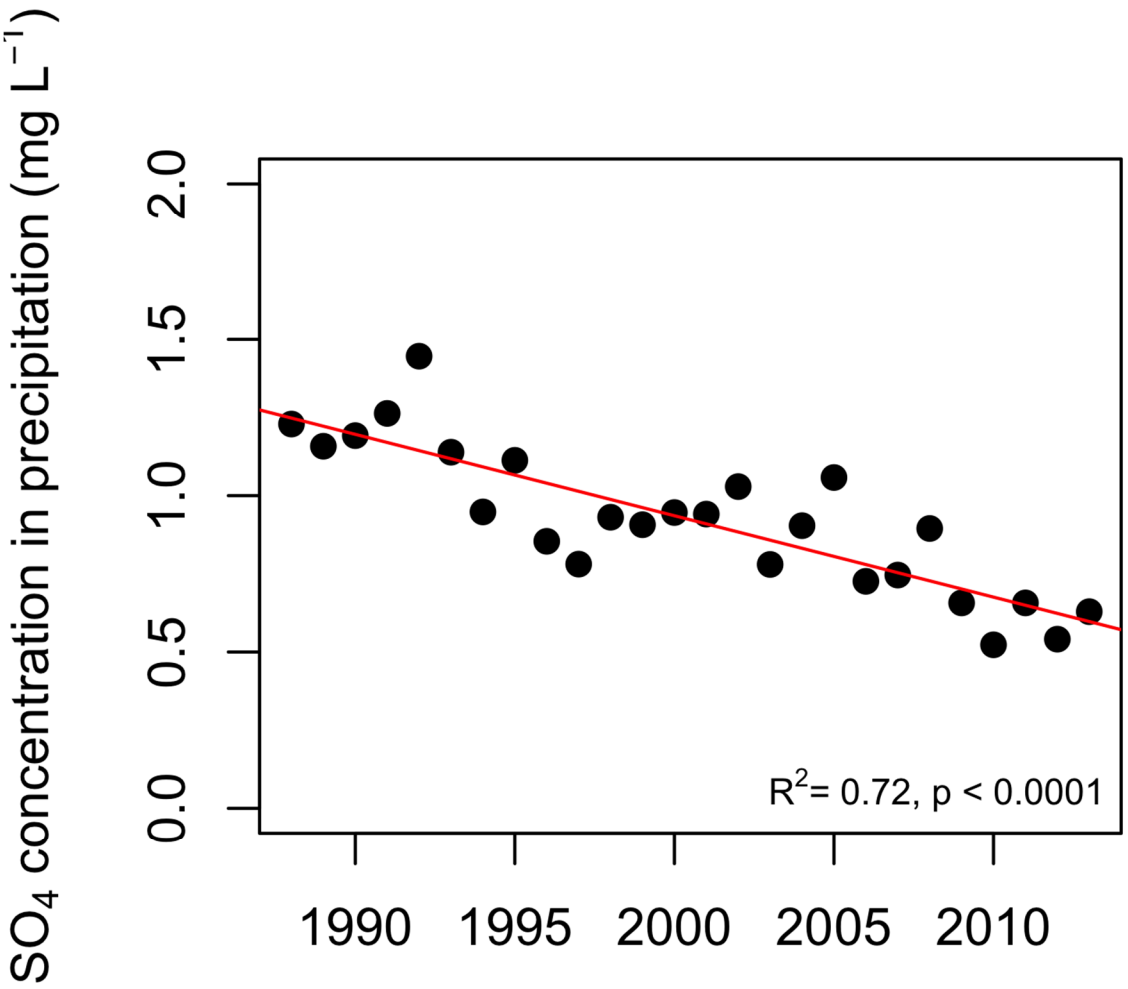

Figure S3: Mean annual SO_4 concentrations declined 0.03 mg L^{-1} Y^{-1} at the National Atmospheric Deposition Program (NADP) site MI99 located 16 km south of the watershed from 1988 - 2013.

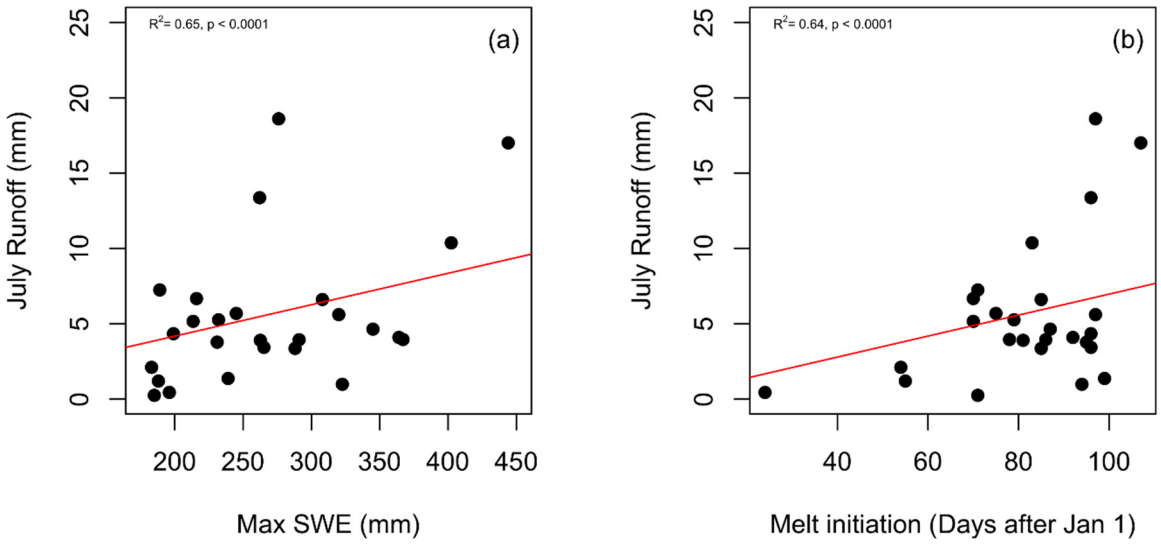

Figure S4: (a) Cumulative July runoff is positively correlated with maximum SWE and (b) Melt initiation date.

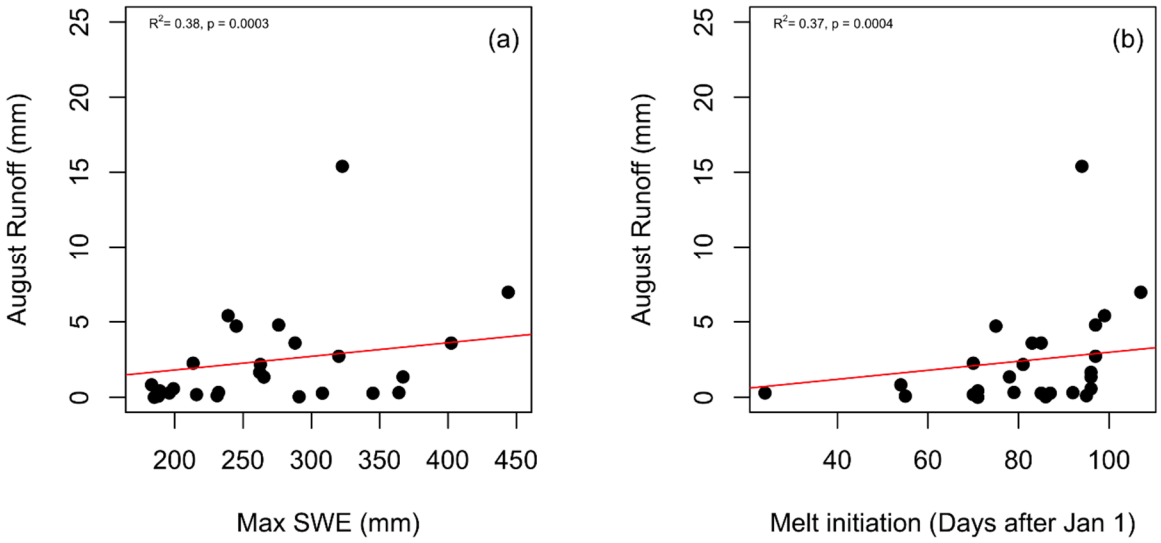

Figure S5: (a) Cumulative August runoff is positively correlated with maximum SWE and (b) Melt initiation date.

2 Seasonal trends of DOM character in leachates, soils, and stream change with snowmelt timing

Karl M. Meingast[1]

Evan S. Kane[1, 2]

Amy M. Marcarelli[3]

Joseph W. Wagenbrenner[4]

[1] Michigan Technological University; College of Forest Resources and Environmental Science; Houghton, MI

[2] U.S.D.A. Forest Service; Northern Research Station; Houghton, MI

[3] Michigan Technological University; Department of Biological Sciences; Houghton, MI

[4] USDA Forest Service, Pacific Southwest Research Station, Arcata, California

2.1 Abstract

Dissolved organic matter (DOM) represents a significant pool of total ecosystem carbon with potential to be translocated from plant materials, through soils, and into aquatic environments. However, exactly how portions of DOM are selectively removed and altered with movement through soils and into streams is not well understood. We studied the optical character of DOM as it moved through a forested watershed, across contrasting aspects with different snowmelt rates, and into a small northern headwater stream. We found significant differences among optical characteristics of leaf leachates,

DOM within soil A and B horizons (spodic horizons) and stream DOM. The largest differences between A and B horizons occurred on north-facing slopes. We measured a seasonal decline in an index of DOM molecular weight and processing (spectral slope, $S_{275\text{-}295}$; range = 0.0102 to 0.0214), a seasonal increase in an index of recently derived DOM (Biological Index, BIX; range = 0.2 to 1.1), and a seasonal decrease in an inverse index of DOM oxidation or diagenesis (ratio of Peak C to Peak A, or C/A; range = 0.59 to 2.010) through snowmelt. These trends in stream character were not influenced by discharge and did not track with hydrograph peaks. The three trends did reflect the differences in character in DOM from the north facing soils which had a more persistent snowpack than DOM from the south aspect soils. C/A displayed unique trends in soil lysimeters and the stream that were not captured with any of the other metrics and were likely reflecting the diagenesis of DOM through the system. The stream appeared humic-like throughout the study period (Humification Index, HIX; mean = 10.9; mean DOC concentration = 4.6 mg C L^{-1}). Overall our study displayed optical changes in DOM translocated from surface litter to deeper mineral soils that changed throughout the progression of snowmelt on different aspects, but these changes did not reflect simultaneous pulses of snowmelt at the watershed scale.

2.2 Introduction

Dissolved organic matter (DOM) represents a significant and mobile carbon pool in the earth's carbon cycle [*Battin et al., 2009*]. Terrestrial DOM is one of the largest

sources of organic carbon delivered to aquatic ecosystems, yet how it is delivered is highly complex [*Tranvik et al., 2009*]. DOM encompasses a broad continuum of organic materials formed by the degradation of terrestrial and microbial inputs. Processing by microbes, interactions with reactive minerals, and abiotic and biotic degradation as these compounds are moved into and through soils can have significant effects on the composition of DOM delivered to aquatic environments [*Kaiser and Kalbitz, 2012; Hutchins et al., 2017*].

Infiltration of precipitation provides a strong mechanism for translocation of DOM through soils [*Kaiser and Kalbitz, 2012; Rothstein et al., 2018*]. In areas where snowmelt dominates the annual hydrograph, infiltration is dominated by contributions from the spring freshet [*Stottlemyer and Toczydlowski, 1991*] and in turn, this results in the largest flushing of DOM from the watershed owing to the large volume of water movement and a high degree of hydrologic connectedness [*e.g., Hornberger et al., 1994; Boyer et al., 1997*]. It is likely that the magnitude of these pulses determines the ability of terrestrially sourced DOM to pass into the mineral horizons, with less alteration [*Rothstein et al., 2018*]. In snowmelt dominated systems, warmer winters associated with a changing climate may be counterintuitively accompanied by wetter, colder soils owing to slower, earlier snowmelt and decreased snow cover to insulate the soil [*Groffman et al., 2001; Musselman et al., 2017*]. As such, changes in the timing of melt will likely affect the degree of infiltration into soils, but there is still much uncertainty as to how

these processes will in turn affect the movement and transformation of DOM from soils to streams.

Regional differences in snow accumulation largely determine the vertical movement of DOM, which in turn influences soil horizon formation in forested watersheds [*Schaetzl and Isard, 1991; 1996*]. The resulting lower incident solar radiation and insolation on north facing aspects leads to a higher degree of infiltration relative to evaporation [*Hunckler and Schaetzl, 1997*]. As such, changes in the amounts and timing of snowmelt exert considerable control over the infiltration of DOM and its transformation and translocation within and among soil horizons.

To understand DOM on its path through the soil-stream continuum, it is helpful to understand the processes involved in soil transformations of DOM. In Spodosols (Podzols), soils formed through illuviation due to infiltration of precipitation, a fraction of DOM from plant materials, such as leaf litter, is stabilized in upper mineral soil horizons [*Kaiser and Guggenberger, 2000*]. The degree to which Spodosols develop, in turn controlling their ability to alter percolating DOM, is controlled by infiltration of precipitation—predominantly snowmelt in north-temperate regions [*Shaetzl et al., 2015; 2018; Rothstein et al., 2018*]. The upper soil horizons, particularly the litter layer, contain relatively young and less processed DOM. These soil and litter-derived pools of DOM are likely the main contributions to streams in forested watersheds and therefore connote distinct characteristics to stream DOM [*McDowell and Wood, 1984; Qualls and Haines, 1992; Burns et al., 2016*]. However, variability in the input of surface-soil derived DOM

to streams can be high depending on the nature of soil flow paths [*Abou Najm et al., 2019*] and factors regulating infiltration, such as snowmelt dynamics [*Boyer et al., 2000*].

The objective of this study was to investigate changes in the character of DOM along continua of formation from leaf litter to different soil horizons, and ultimately its export to a stream, with variation in the timing of snowmelt. We measured DOM from north and south facing aspects with different snowmelt dynamics in the same watershed, and compared these with seasonal trends in stream DOM character. We hypothesized that peak stream flows during snowmelt would be associated with changes in DOC concentrations and optical character in the stream. Furthermore, we hypothesized that DOM variation would be evident between A and B soil horizons, between north and south aspects, as well as between soils and the stream when analyzed with absorption and fluorescence spectroscopy. We also expected to see shifts in the stream DOM quantity and character corresponding with seasonal changes in the connectivity of soils and the stream on north vs. south aspects, owing to changes in the timing of snowmelt and degree of spodic soil horizon development.

2.3 Materials and Methods

2.3.1 Study site characterization

Brooks Gorge Research Watershed (BGRW) is located 6 km northwest of Michigan Technological University (47.1601, -88.6273) in the Upper Peninsula of Michigan (Figure 1). The region receives an average of 828 mm of precipitation annually (1983 –

2018; National Atmospheric Deposition Program; MI99), with an average peak snow water equivalent of 271 mm (range of 183 to 444 mm) [*Chapter 1*]. The watershed is predominantly oriented east to west, causing north to south aspect contrasts (Figure 1). The lower portion of the stream (L, Gauge) supports year-round flow, while the upper portion (U) is intermittent. The watershed forest cover is mixed northern hardwoods, dominated by *Acer saccharum* (Marsh.), *Acer rubrum* (L.), *Tilia Americana* (L.), *Betula alleghaniensis* (Britton), *Quercus rubra* (L.) and *Ostrya virginiana* (Mill.). The soils are described as a complex of Oxyaguic Fragiorthods (Graveraet Series) and Typic Haplorthods (Kalkaska Series). Spodic horizons are more developed on the north facing aspects, with B horizons having average thicknesses of 45 cm and 29 cm on north and south facing aspects, respectively (Table S1; Figure S1).

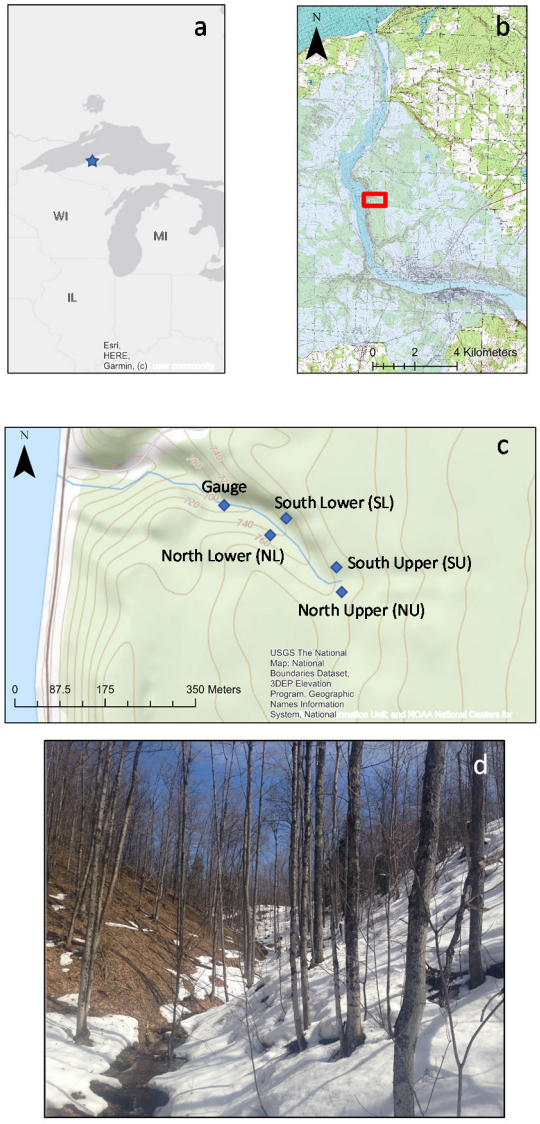

Figure 1: (a) The location of BGRW study site in the Upper Peninsula of Michigan. (b) The location of BGRW in relation to the Portage Shipping Canal and Lake Superior. (c) The study site plot layout at BGRW. (d) BGRW on March 29, 2016, highlighting the snowpack differences across aspects. The south facing slope was nearly snow free while the north facing slope held an average snow depth of 25.7 cm.

2.3.2 Leaf leachates Study site characterization

Leaf leachates were collected to establish a fresh DOM endmember signal to the analysis. Leaf leachates for three species, *Acer saccharum* (Marsh.), *Betula papyrifera* (Marsh.) and *Quercus rubra* (L.) were collected in triplicate, twice in November after leaf fall. 5 mg of fresh litter was allowed to steep in 250 ml of MilliQ water for 4 hrs at 4° C. Samples were filtered through 0.7 μm GF/F (Whatman) followed by 0.45 μm nylon membrane filters (Whatman).

2.3.3 Stream and soil water characterization

Stream samples were collected from just prior to melt onset (March 11, 2016) to summer baseflow (June 2, 2016) at three sampling locations along the reach (upper (U), lower (L), and gauge). Soil pore-water was collected over the same period using porous cup tension lysimeters with approximately 50 centibars of vacuum applied (Soil Moisture Corporation; Santa Barbara, CA) corresponding to each of the upper stream sampling locations. Two lysimeters were inserted to each depth (15 cm and 30 cm) on each aspect corresponding to the two stream sampling locations (Figure 1). These depths were chosen to sample lower A horizon and lower B horizon DOM. Pore-water and stream samples were immediately filtered through 0.45 μm PVDF syringe filters into brown HDPE bottles and transported back to the laboratory for further analysis or freezing within 24 hrs.

Stream stage height was measured from March 11 to May 25 with a Solinst Levellogger 3001 and barometrically corrected with a Barologger 3001 (Solinst; Georgetown, ON). Stage height was converted to discharge through the development of a rating curve that was developed by directly intercepting flow with a 26 L container at a constrained point [*Brooks et al., 2013*] (Figure S2). Soil volumetric moisture content (VWC) was measured at Lower stations every 30 minutes using ECH_20 moisture probes (Meter Environment; Pullman, WA). Soil moisture probes were calibrated with gravimetric soil moisture data obtained using fixed-volume corers at the same depths, obtained within 10 m of the stations. Data reported are an average of 15 and 30 cm depths. Air temperature was also recorded at Lower stations for both aspects using Onset TMC6-HD temperature sensors recorded with 4-Channel External HOBO loggers on 30-minute timesteps (Onset Corporation; Bourne, MA). Soil moisture and air temperature were measured from March 11, 2016 to April 30, 2016. North facing air temperatures were only recorded until April 26, 2016. Snow water equivalent (SWE) was measured using a Federal Snow Sampler. Snow cores were weighed with a Brecknell ElectroSamson scale (Brecknell; Fairmont, MN) until each station was snow free.

2.3.4 Chemical and optical analyses

Absorption and fluorescence spectra were analyzed using a Horiba Aqualog fluorometer (Horiba–Jobin–Yvon Aqualog C; Horiba Co., Edison, NJ) in 1 cm quartz cells (Starna Cells, Inc). Absorption spectra were run from 240 nm to 600 nm at 3 nm resolution. Fluorescence spectra were recorded at 3 nm excitation wavelengths from 240 nm to 600

nm and emission was recorded at 3 nm resolution from 240 nm to 640 nm (Figure S3). Fluorescence spectra were converted to Raman units (R.U.) using Raman scattering from a sealed Milli-Q cuvette (Starna) (R.U.) *[Lawaetz and Stedmon, 2009*]. Absorbance values were converted to Naperian absorption coefficients (a_λ) [*Green and Blough, 1994*]:

$$a_\lambda = 2.303 \frac{A_\lambda}{L} \quad (1)$$

Where A_λ is absorbance at wavelength λ, and L is the path-length, in meters. Inner filter effects, Raman scattering, and Raleigh scattering for fluorescence EEMs were accounted for using the PLS toolbox (version 782; Eigenvector) in Matlab (r2014a). We derived two specific spectral slopes ($S_{275\text{-}295}$ and $S_{350\text{-}400}$) from the absorption spectra as indicators of average DOM molecular weight [*Helms et al., 2008*], and these were calculated as the slopes of the linear regressions of log-transformed absorption spectra from 275-295 nm and 350-400 nm, respectively.

We derived three parameters from the fluorescence spectra. The biological index (BIX), used to differentiate terrestrial reference standards from phytoplankton derived DOM [*Osburn et al., 2019*] and humification index (HIX), an index of soil humification [*Zolsnay et al., 1999; Ohno, 2002*] and were defined as:

$$BIX = \frac{F_{380}}{F_{430}} \text{ (at excitation of 310 nm)} \quad (2)$$

Where F_{380} and F_{430} are the fluorescence emission intensities at 380 and 430 nm, respectively (at excitation 310 nm).

$$HIX = \frac{\Sigma F_{435-480}}{\Sigma F_{300-345}} \text{ (at excitation of 254 nm)} \quad (3)$$

Where $\Sigma F_{435-480}$ is the sum of the fluorescence emission from 435 to 480 nm and $\Sigma F_{300-345}$ is the sum of the fluorescence emission from 300 – 345 nm.

Additionally, the ratio of fluorescence Peak C to Peak A (C/A), which has been shown to inversely track photodegradation of DOM [*Coble, 1996; Hansen et al. 2016*] as well as the degree of humic substance degradation or oxidation [*Moran et al., 2000; Kothawala et al., 2012*] was calculated as:

$$C/A = \frac{F_{ex340/em440}}{F_{ex260/em450}} \quad (4)$$

All samples were acidified to pH 2 with HCl (VWR) and analyzed for total organic carbon with a Shimadzu TOC-V analyzer (Shimadzu; Kyoto, Japan). We report the specific absorbance normalized by DOC concentration of the sample ($SUVA_{254}$) as a metric to quantify the amount of chromophoric DOM in the sample, which has also been related to DOM aromaticity [*Weishaar et al., 2003*].

2.3.5 Statistics

A one-way analysis of variance (ANOVA) with a Tukey's honest significant difference (HSD) test was used to assess mean differences in absorption and fluorescence indices between sampling locations. Linear regression was used in conjunction with non-parametric Mann Kendall trend analysis to analyze trends in stream DOC concentrations as well as absorption and fluorescence indices through time in R [v3.0.3; R Core Team, 2014].

2.4 Results

2.4.1 Hydrology

Snowpack measured at the onset of this study was similar between north and south aspects (Figure 2a) with maximum SWE of 170 mm and 140 mm on the north and south facing aspects, respectively. Snowpack melted much more rapidly on the south facing slopes, rendering them snow free about one month before the north slopes (e.g., Figure 1d). Air temperatures exhibited a wide range, from -12°C to 28°C on the south facing aspect and -11 °C to 25 °C on the north aspect. Both aspects followed similar diurnal trends in temperature (Figure 2b). Soil VWC of the top 30 cm ranged from 0.30 $cm^3\ cm^{-3}$ to 0.31 $cm^3\ cm^{-3}$. Soil VWC slowly declined over the course of the study period for the south aspect (Mann Kendell trend test; $p < 0.001$) but was relatively constant on the north aspect (Mann Kendell trend test; $p = 0.13$). Stream discharge peaked at 0.180

$m^3 s^{-1}$ on April 15 (DOY 106), far exceeding all other runoff events during the study period (Figure 2).

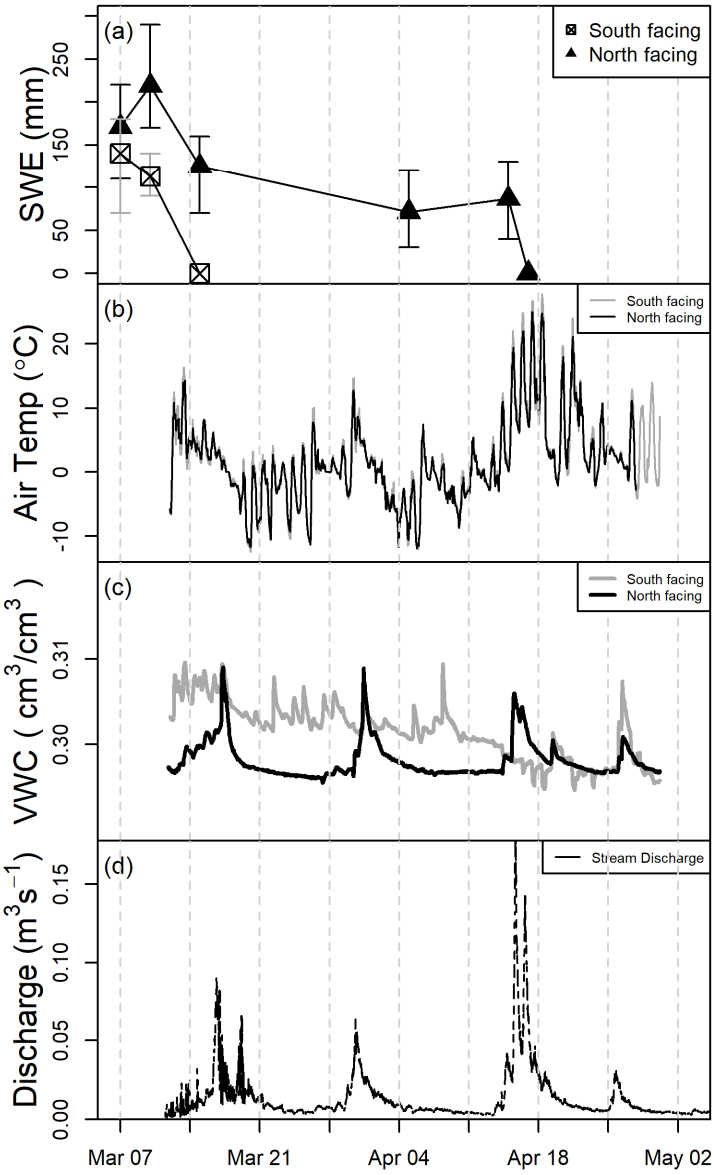

Figure 2: (a) SWE with the range of five sampling locations represented as error bars (b) air temperatures, (c) volumetric water content (VWC) for the top 30 cm of soil and (d) stream discharge over the course of the study period.

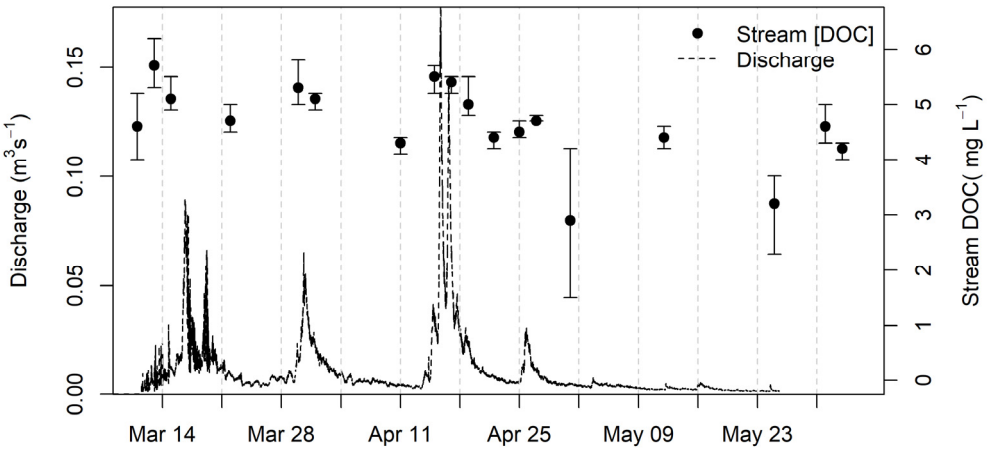

Figure 3: Stream discharge and stream DOC concentrations over the study period. Error bars indicate the range of the three stream sampling locations.

2.4.2 DOC characteristics

Stream DOC concentrations ranged from 2.3 to 5.9 mg L^{-1} with a mean of 4.6 mg L^{-1} (Figure 3). There were no significant trends in stream DOC concentration with time or discharge. Soil lysimeter DOC concentrations ranged from 11.0 to 79.3 mg L^{-1} (S.E. = 4.5 mg L^{-1}) on the north aspect and 7.6 to 76.1 mg L^{-1} (S.E. = 4.8 mg L^{-1}) on the south aspect. There was not a significant difference in DOC concentrations across aspects. Neither aspect displayed a significant trend in DOC concentration.

2.4.3 Absorption metrics

$SUVA_{254}$, an index of aromaticity, was variable and ranged from 0.62 to 4.86 in leaf leachates. $SUVA_{254}$ ranged from 1.2 to 3.6 in the stream and did not show a significant trend through time. Stream $SUVA_{254}$ was significantly lower than all soil lysimeter locations except north-facing 30 cm lysimeters (Table 1).

$S_{275\text{-}295}$, an indicator of average DOM molecular weight, was most variable in leaf leachates where it ranged from 0.0102 to 0.0200. $S_{275\text{-}295}$ ranged from 0.0145 to 0.0189 in the stream, 0.0115 to 0.0154 on the south facing aspect and 0.0118 to 0.0214 on the north facing aspect (Figure 4a). Leaf leachate $S_{275\text{-}295}$ values were not statistically different from north facing 15 cm lysimeters, and were significantly different from all other locations (Table 1). $S_{275\text{-}295}$ in all soil locations except for the north facing 30 cm lysimeters were significantly different from the stream values (Table 1). There was a significant increase in the stream $S_{275\text{-}295}$ through the study period. $S_{275\text{-}295}$ showed no trend through time for lysimeters from either aspect (Figure 4a).

$S_{350\text{-}400}$, another indicator of average DOM molecular weight, ranged from 0.0139 to 0.0268 in leaf leachates. $S_{350\text{-}400}$ ranged from 0.0134 to 0.0590 in the stream, 0.0165 to 0.0363 on the south facing aspect and 0.0161 to 0.0407 on the north facing aspect (Figure 4b). $S_{350\text{-}400}$ was not significantly different between aspects (Table 1) and showed no time trends at any location, though there was an increase on March 28 coincident with a hydrograph peak on March 29 (Figure 4b; Figure 3).

2.4.4 Fluorescence metrics

HIX, an index of DOM humification, ranged from 0.5 to 2.0 in leaf leachates. HIX ranged from 6.4 to 15.6 in the stream, 6.6 to 34.1 on the south facing aspect and 3.7 to 25.7 on the north facing aspect (Figure 4c). HIX was similar between north facing 30 cm lysimeters and stream, however, all other lysimeter locations were significantly different (higher) than the stream (Table 1). 15 cm lysimeters were significantly different between aspects, however 30 cm south facing lysimeters were not significantly different from either 15 cm location. There were no time trends in HIX.

BIX, an index used to differentiate Suwannee River Fulvic Acid (SRFA) from phytoplankton derived DOM [*Osburn et al.,* 2019], ranged from 0.2 to 1.1 in leaf leachates. BIX ranged from 0.5 to 0.6 in the stream, 0.4 to 0.6 on the south facing aspect and 0.4 to 0.8 on the north facing aspect (Figure 4d). Similar to HIX, BIX values from north-facing 30 cm lysimeters were similar to the stream while all other lysimeter locations were different (Table 1). The south aspect showed a decrease in BIX through time, while BIX in the stream increased (Figure 4d).

The ratio of fluorescence Peak C to Peak A (C/A), which has been shown to inversely relate to photodegradation or degree of biodegradation, ranged from 0.99 to 2.01 in leaf leachates. C/A ranged from 0.62 to 0.74 in the stream, 0.57 to 0.99 on the south facing aspect and 0.59 to 0.89 on the north facing aspect (Figure 4e). C/A in the stream was significantly different than all lysimeter locations except 30 cm south facing

lysimeters (Table 1). Both the north aspect and stream showed decreasing trends through time in C/A.

Table 1: Absorption and fluorescence indices (mean and standard error) from leaf leachates, soil lysimeters and stream water. Letters indicate significant differences

between locations. Number of samples (n) for $SUVA_{254}$ is reported as it varied compared to other metrics.

Location	$SUVA_{254}$ (L mg C^{-1} m^{-1})	$S_{275-295}$	$S_{350-400}$	HIX	BIX	C/A
Leaf leachates *(n = 18)*	2.5(0.3)^{a} (n = 18)	0.0147(0.0006)^{a}	0.0172(0.0007)^{a}	1.0(0.1)^{a}	0.39(0.05)^{a}	1.38(0.07)^{a}
North-facing 15 cm lysimeters *(n = 24)*	7.1(1.3)^{b} *(n = 12)*	0.0136(0.0003)^{a,b}	0.0220(0.0024)^{a}	14.6(0.9)^{b}	0.48(0.01)^{b}	0.75(0.02)^{b}
North-facing 30 cm lysimeters *(n = 24)*	3.6(0.3)^{a} *(n = 11)*	0.0160(0.0003)^{c}	0.0214(0.0010)^{a}	10.6(1.2)^{d}	0.62(0.01)^{c}	0.74(0.01)^{b}
South-facing 15 cm lysimeters *(n = 28)*	6.3(1.1)^{b}*(n = 17)*	0.0133(0.0002)^{b}	0.0191(0.0003)^{a}	19.1(1.3)^{c}	0.46(0.01)^{a,b}	0.73(0.02)^{b}
South-facing 30 cm lysimeters *(n = 27)*	7.7(1.9)^{b} *(n= 19)*	0.0136(0.0002)^{b}	0.0204(0.0009)^{a}	17.2(1.0)^{b,c}	0.50(0.01)^{b}	0.72(0.01)^{b,c}
Stream *(n = 77)*	2.8(0.1)^{a} *(n = 56)*	0.0161(0.0001)^{c}	0.0200(0.0007)^{a}	10.9(0.2)^{d}	0.59(0.03)^{c}	0.66(0.004)^{c}

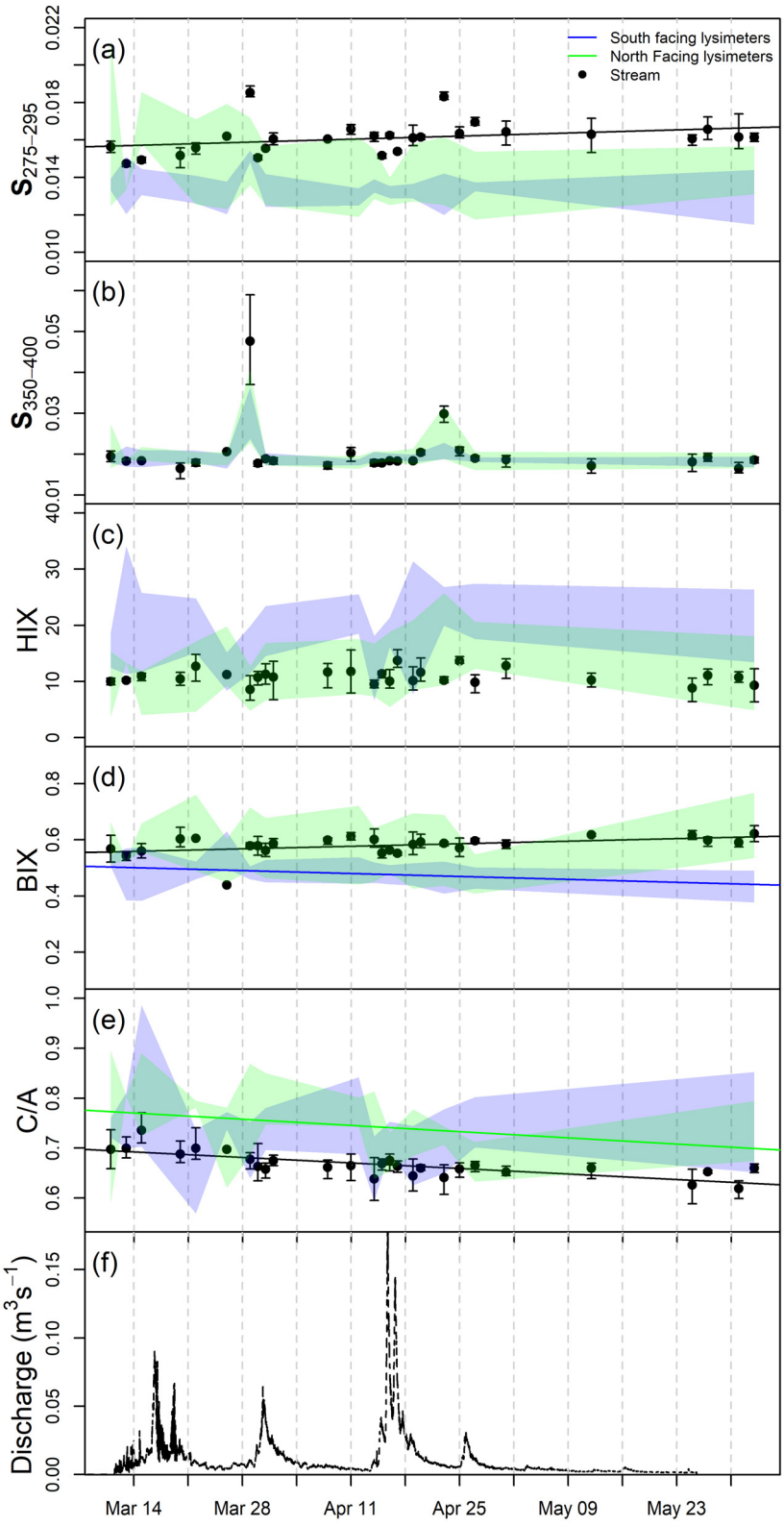
South facing lysimeters
North Facing lysimeters
Stream
(a)
$S_{275-295}$
0.010
0.014
0.018
0.022
(b)
$S_{350-400}$
0.01
0.03
0.05
(c)
HIX
0
10
20
30
40
(d)
BIX
0.2
0.4
0.6
0.8
1.0
(e)
C/A
0.6
0.7
0.8
0.9
1.0
(f)
Discharge (m^3s^{-1})
0.00
0.05
0.10
0.15
Mar 14
Mar 28
Apr 11
Apr 25
May 09
May 23

Figure 4: Soil lysimeter and stream absorption and fluorescence metrics through the study period. Regression lines represent significant trends in time. (a) $S_{275\text{-}295}$; (b) $S_{350\text{-}400}$; (c) HIX; (d) BIX; (e) C/A; and (f) Stream discharge over the study period. Error bars indicate the range of the three stream sampling stations. Shaded regions represent the ranges of lysimeter water from north and south aspects.

2.5 Discussion

2.5.1 Aspect influence on snowmelt dynamics

Snowpack melted quicker on the south facing aspect with no apparent pulse in soil moisture (Figure 2). Similarity in air temperatures between aspects indicate the importance of solar radiation on the snowmelt rates between aspects (Figure 2b). Soil moisture was constant through time with periodic wetting pulses on the north aspect, corresponding with stream hydrograph peaks, whereas the south aspect soil moisture showed a decline over time (Figure 2c). The varying trends between aspects demonstrate the different soil wetting regimes through the melt, which are also manifest in the increased podzolization in the north aspect soils [*Hunckler and Schaetzl, 1993; Shaetzl and Isard, 1996; Shaetzl et al., 2018*]. Together, these factors suggest a higher degree of hydrologic connectivity between north aspect soils and the stream, and highlight the importance of a persistent snowpack for the mobility of DOM.

2.5.2 How does stream DOM track with snowmelt?

Contrary to our hypothesis, stream DOC concentrations did not track the snowmelt hydrograph (Figure 3). This is a direct contrast from a previous study in an alpine watershed exhibiting a snowmelt-dominated hydrograph with similar magnitude of discharge and seasonal DOC concentrations [*Burns et al., 2016*]. We attribute the different responses in DOC concentrations to snowmelt dynamics to the different soil types present. In the Burns et al. [*2016*] study, north aspect soils were Inceptisols (a complex of Dystrocryepts and Haplocryepts) and south aspect soils were also poorly developed and shallow (lithic). In contrast the Spodosols of our study, which exhibit spodic horizons and organic carbon accumulation truncated near the surface, could moderate DOC flushing to the stream from deeper within the soil profile. Moreover, surface-litter derived DOM dominates the character of mineral soil horizon DOM in Spodosols [*Rothstein et al., 2018*], which offers a parsimonious explanation for the much higher HIX values in our stream (mean HIX = 10.9) compared with the study described in *Burns et al.,* [*2016*] (minimum HIX = 1.80; maximum HIX = 3.85). Taken together, these findings demonstrate that streams with very similar snowmelt-dominated hydrographs can exhibit quite different DOM composition and export characteristics, as determined by soil properties.

Hydrograph driven changes were not apparent in stream DOM character in this study, even when north aspect soil moisture trends strongly resembled the stream hydrograph (Figure 3, Figure 4). The exceptions to this were the two spectral slope

metrics ($S_{275-295}$, $S_{350-400}$) and BIX, which increased and decreased, respectively, in conjunction to the second hydrograph peak (Figure 4). These findings indicated a consistent degree of processing for the DOM delivered to the stream through snowmelt, regardless of soil wetting. Interestingly, metrics concretely associated with DOM degradation displayed gradual trends towards increased degradation through time in the stream ($S_{275-295}$, C/A, BIX). The decline in C/A over time suggests a change in the DOM pool to one which is more degraded or oxidized, which is consistent with prior work showing the decline in C/A in long-term incubations of lake water [*Kothawala et al.,* 2012], as well as with the photodegradation of soil and plant leachates [*Hansen et al., 2016*].

These trends in DOM degradation over time do not necessarily follow hydrograph peaks or wetting pulses, but could be tracking changes in DOM composition by aspect. For example, $S_{275-295}$ and BIX showed significant differences between A and B horizons on the north aspect (Table 1). Trends in $S_{275-295}$, C/A and BIX could be tracking an increasing hydrologic disconnection between south aspects and stream as the south aspect gradually dried out (Figure 2). On the other hand, BIX and C/A measured in the stream tracked BIX and C/A in the north aspect soils throughout the study (Figure 4). These trends are consistent with asynchronous snowmelt occurring on different landscape positions, and therefore gradual shifts in the timing of DOM contributions from different sources to the stream through snowmelt [*cf. Boyer et al., 2000*]. However, different

optical properties of DOM vary in their accurate reflection of these different DOM sources to the stream with the progression of snowmelt.

2.5.3 How does DOC vary optically between leaf leachates, A and B horizons?

Leaf leachates displayed unique optical character as compared to soil A and B horizons and stream water. However, these differences were not consistently reflected in all metrics. For example, $SUVA_{254}$ was similar between leaf leachates, north facing B horizon, and the stream, while $S_{275\text{-}295}$ displayed significant differences among these sample locations. However, the general trend of low $SUVA_{254}$ corresponding to high $S_{275\text{-}295}$ [*Helms et al., 2008*] was observed in this study.

$S_{350\text{-}400}$ was similar in leachates, all soils, and the stream. The decoupling of $S_{350\text{-}400}$ from $S_{275\text{-}295}$ was likely due to the decreased sensitivity of $S_{350\text{-}400}$ to DOM degradation [*Helms et al., 2008; Helms et al., 2013*]. However, $S_{350\text{-}400}$ showed changes corresponding to a snowmelt peak, indicating this metric is responsive to hydrologic changes in this system, and indicating its ability to track a specific DOM transformation not as evident through $S_{275\text{-}295}$. Overall, the soil-stream interface provides an opportunity to examine unique controls on $S_{350\text{-}400}$ and $S_{275\text{-}295}$, as they appear decoupled in this environment (Table 1). This is a unique finding as previous studies have reported these two slopes to generally track together [*Helms et al., 2008; Hansen et al., 2016*].

HIX was the only fluorescence metric which differentiated A horizon DOM between aspects (Table 1). South facing 30 cm lysimeters (B horizon) were not differentiated from A horizon soils in any metric, yet B horizons in north facing soils displayed significantly different $SUVA_{254}$, $S_{275\text{-}295}$, HIX and BIX from A horizon lysimeters. Because B horizon DOM characteristics were also significantly different than leaf leachates for $S_{275\text{-}295}$, HIX, BIX and C/A, we hypothesize that B horizon DOM was not simply translocated from surface horizons, but more processed DOM as a result of its residence time in the A horizon and preferential removal of aromatic lignin derivatives through metal complexing in these soils [*Kaiser and Guggenberger, 2000*]. In support of this, soil HIX increased on both aspects through the snowmelt period, further deviating from leaf litter HIX values (Figure 4). Because HIX values diverged from litter sources, we hypothesize within soil processing of fresh inputs was likely responsible for these high HIX values.

C/A displayed a unique trend as compared to all other indices (Table 1; Figure 4). C/A was the only metric to show a consistently declining trend from leaf leachates, to A and B horizons, and finally to the stream. Both C and A peaks are within the humic-like region of fluorescence, and the peaks are likely tracking a similar fraction of DOM [*Coble, 1996; Hansen et al., 2016*]. Given this, we postulate that C/A (particularly peak C) was tracking a consistent humic-like DOM fraction of compounds through our study which was: (1) not easily adsorbed by soils or biologically removed, (2) not strongly influenced by processes altering HIX, BIX or spectral slopes, and (3) representing a

fraction whose fluorescence was able to directly or indirectly be altered within soils. Given these factors, we suggest that C/A in our study was tracking partial oxidation of lignin-like derivatives from the humic-like DOM pool which was sourced from inputs such as leaf litter and yet not easily adsorbed by soils. Previous research using long-term incubations of lake water under dark conditions showed the selective removal of peak C relative to peak A, thus suggesting biodegradation and not photooxidation [*Kothawala et al., 2012*]. If C/A were tracking a selective removal of a different DOM fraction, likely hydrophobic acids in Spodosols [*Dai et al., 1996*], we would expect the B horizons of the more developed north aspect soils to display the lowest values of C/A. However, B horizons on the south aspect displayed the lowest C/A values. Our study suggests that C/A may be the most applicable metric for tracking the diagenesis of the translocated DOM. We hypothesize C/A is likely tracking hydrophilic acid and/or hydrophilic neutral fractions [*Qualls and Haines, 1991*], which is consistent with Kothawala et al. [2012], who found inconsistent changes in incubated DOM character using other spectral indexes Indices such as $SUVA_{254}$, $S_{275\text{-}295}$, HIX and BIX are likely altered by removal of DOM fractions but it is not clear if these indices reflect changes in specific pools of DOM or rather are tracking changes in bulk DOM. Further work examining the extent to which these indices track alteration of specific sources of DOM as opposed to selective loss of fluorophores is needed to extend the application of these indices as tracers of DOM in the terrestrial-aquatic interface. The varying trends over time through soil profiles and into the stream illustrate some of the difficulties of using optical metrics to infer source of DOM [*cf. Burns et al. 2016*]. Overall, this study highlights the utility of fluorescence and

absorption spectroscopy in understanding seasonal changes in DOM properties at the terrestrial-aquatic interface. We found fluorescence metrics, specifically C/A, to add additional insights into DOM diagenesis through soils and into streams which were not evident in absorption measurements. Future work combining mass spectroscopy in probing the response of these DOM fractions to borohydride reduction of ketone and aldehyde functional groups [*Andrew et al., 2013; Osburn et al., 2019*] could further distinguish the source of B horizon DOM, and its diagenesis, by tracking partial oxidation of ketones and aldehydes to carboxylic acids.

2.5.4 What are the implications under a changing climate?

Anticipated changes in the climate of northern regions are likely to lead to earlier and more prolonged snowmelt [*Musselman et al., 2017*]. In lake effect snow dominated areas, which are also coincident with high spodic soil horizon development, it is unlikely that winter snowpack will decrease enough to uncouple water in soils and streams during snowmelt [*Chapter 1*]. Perhaps counterintuitively, the north-aspects described in this study could be analogous to these earlier, slower and more prolonged melt patterns. Earlier snowmelt during periods with lower sun angles and less incident solar radiation would increase wetting pulses in soils (e.g. north aspect; Figure 2c). These factors are likely to increase the vertical movement of DOM (spodic soil horizon development) as well as increase the fraction of less humic-like (lower HIX) and lower molecular weight (higher $S_{275\text{-}295}$) character in DOM reaching the stream.

2.6 References

Abou Najm, M., Lassabatere, L. and Stewart, R.D., 2019. Current Insights into Nonuniform Flow across Scales, Processes, and Applications. *Vadose Zone Journal*, *18*(1), p.190113.

Andrew, A. A., Del Vecchio, R., Subramaniam, A., & Blough, N. V. (2013). Chromophoric dissolved organic matter (CDOM) in the Equatorial Atlantic Ocean: optical properties and their relation to CDOM structure and source. *Marine Chemistry*, *148*, 33-43.

Battin, T. J., Luyssaert, S., Kaplan, L. A., Aufdenkampe, A. K., Richter, A., & Tranvik, L. J. (2009). The boundless carbon cycle. *Nature Geoscience*, *2*(9), 598-600.

Boyer, E. W., Hornberger, G. M., Bencala, K. E., & McKnight, D. M. (1997). Response characteristics of DOC flushing in an alpine catchment. *Hydrological processes*, *11*(12), 1635-1647.

Boyer, E. W., Hornberger, G. M., Bencala, K. E., & McKnight, D. M. (2000). Effects of asynchronous snowmelt on flushing of dissolved organic carbon: a mixing model approach. *Hydrological processes*, *14*, 3291-3308.

Brooks, K. N., Ffolliott, P. F., Magner, J. A. (2013). Hydrology and the Management of Watersheds- 4th Edition. John Wiley and Sons, Inc. pp. 141-144.

Burns, M. A., Barnard, H. R., Gabor, R. S., McKnight, D. M., & Brooks, P. D. (2016). Dissolved organic matter transport reflects hillslope to stream connectivity during snowmelt in a montane catchment. *Water Resources Research*, *52*(6), 4905-4923.

Coble, P. G. (1996). Characterization of marine and terrestrial DOM in seawater using excitation-emission matrix spectroscopy. *Marine chemistry*, *51*(4), 325-346.

Dai, K. O. H., David, M. B., Vance, G. F., & Krzyszowska, A. J. (1996). Characterization of phosphorus in a spruce-fir spodosol by phosphorus-31 nuclear magnetic resonance spectroscopy. *Soil Science Society of America Journal*, *60*(6), 1943-1950.

Green, S. A., & Blough, N. V. (1994). Optical absorption and fluorescence properties of chromophoric dissolved organic matter in natural waters. *Limnology and Oceanography*, *39*(8), 1903-1916.

Groffman, P. M., Driscoll, C. T., Fahey, T. J., Hardy, J. P., Fitzhugh, R. D., & Tierney, G. L. (2001). Colder soils in a warmer world: a snow manipulation study in a northern hardwood forest ecosystem. *Biogeochemistry*, *56*(2), 135-150.

Hansen, A. M., Kraus, T. E., Pellerin, B. A., Fleck, J. A., Downing, B. D., & Bergamaschi, B. A. (2016). Optical properties of dissolved organic matter (DOM): Effects of biological and photolytic degradation. *Limnology and Oceanography*, *61*(3), 1015-1032.

Helms, J. R., Stubbins, A., Ritchie, J. D., Minor, E. C., Kieber, D. J., & Mopper, K. (2008). Absorption spectral slopes and slope ratios as indicators of molecular weight, source, and photobleaching of chromophoric dissolved organic matter. *Limnology and Oceanography*, *53*(3), 955-969.

Helms, J. R., Stubbins, A., Perdue, E. M., Green, N. W., Chen, H., & Mopper, K. (2013). Photochemical bleaching of oceanic dissolved organic matter and its effect on absorption spectral slope and fluorescence. *Marine Chemistry*, *155*, 81-91.

Hornberger, G. M., Bencala, K. E., & McKnight, D. M. (1994). Hydrological controls on dissolved organic carbon during snowmelt in the Snake River near Montezuma, Colorado. *Biogeochemistry*, *25*(3), 147-165.

Hunckler, R. V., & Schaetzl, R. J. (1997). Spodosol development as affected by geomorphic aspect, Baraga County, Michigan. *Soil Science Society of America Journal*, *61*(4), 1105-1115.

Hutchins, R. H., Aukes, P., Schiff, S. L., Dittmar, T., Prairie, Y. T., & del Giorgio, P. A. (2017). The optical, chemical, and molecular dissolved organic matter succession along a boreal soil-stream-river continuum. *Journal of Geophysical Research: Biogeosciences*, *122*(11), 2892-2908.

Kaiser, K., & Guggenberger, G. (2000). The role of DOM sorption to mineral surfaces in the preservation of organic matter in soils. *Organic geochemistry*, *31*(7-8), 711-725.

Kaiser, K., & Kalbitz, K. (2012). Cycling downwards–dissolved organic matter in soils. *Soil Biology and Biochemistry*, *52*, 29-32.

Kothawala, D. N., Wachenfeldt, E. v., Koehler, B., Tranvik, L. J. (2012). Selective loss and preservation of lake water dissolved organic matter fluorescence during long-term dark incubations. *Science of the Total Environment, 433,* 238-246.

Lawaetz, A. J., & Stedmon, C. A. (2009). Fluorescence intensity calibration using the Raman scatter peak of water. *Applied spectroscopy*, *63*(8), 936-940.

McDowell, W. H., Wood, T. (1984). Podzolization: soil processes control dissolved organic carbon concentrations in stream water.

Moran. M. A., Sheldon, W. M., Zepp, R.G. (2000). Carbon loss and optical property changes during long-term photochemical and biological degradation of estuarine dissolved organic matter. *Limnology and Oceanography, (45)*, 1254–64.

Musselman, K. N., Clark, M. P., Liu, C., Ikeda, K., & Rasmussen, R. (2017). Slower snowmelt in a warmer world. *Nature Climate Change*, *7*(3), 214-219.

Ohno, T. (2002). Fluorescence inner-filtering correction for determining the humification index of dissolved organic matter. *Environmental science & technology*, *36*(4), 742-746.

Osburn, C. L., Kinsey, J. D., Bianchi, T. S., & Shields, M. R. (2019). Formation of planktonic chromophoric dissolved organic matter in the ocean. *Marine Chemistry*, *209*, 1-13.

Qualls, R. G., & Haines, B. L. (1991). Geochemistry of dissolved organic nutrients in water percolating through a forest ecosystem. *Soil Science Society of America Journal*, *55*(4), 1112-1123.

Qualls, R. G., & Haines, B. L. (1992). Biodegradability of dissolved organic matter in forest throughfall, soil solution, and stream water. *Soil Science Society of America Journal*, *56*(2), 578-586.

R Core Team (2014). R: A language and environment for statistical computing. R Foundation for Statistical Computing, Vienna, Austria. URL http://www.R-project.org/.

Rothstein, D. E., Toosi, E. R., Schaetzl, R. J., & Grandy, A. S. (2018). Translocation of carbon from surface organic horizons to the subsoil in coarse-textured Spodosols: implications for deep soil C dynamics. *Soil Science Society of America Journal*, *82*(4), 969-982.

Schaetzl, R. J., & Isard, S. A. (1991). The distribution of Spodosol soils in southern Michigan: A climatic interpretation. *Annals of the Association of American Geographers*, *81*(3), 425-442.

Schaetzl, R. J., & Isard, S. A. (1996). Regional-scale relationships between climate and strength of podzolization in the Great Lakes region, North America. *Catena*, *28*(1-2), 47-69.

Schaetzl, R. J., Luehmann, M. D., & Rothstein, D. (2015). Pulses of podzolization: The relative importance of spring snowmelt, summer storms, and fall rains on Spodosol development. *Soil Science Society of America Journal*, *79*(1), 117-131.

Schaetzl, R. J., Rothstein, D. E., & Samonil, P. (2018). Gradients in lake effect snowfall and fire across northern Lower Michigan drive patterns of soil development and carbon dynamics. *Annals of the American Association of Geographers*, *108*(3), 638-657.

Stottlemyer, R. and Toczydlowski, D., 1991. Stream chemistry and hydrologic pathways during snowmelt in a small watershed adjacent Lake Superior. *Biogeochemistry*, *13*(3), pp.177-197.

Tranvik, L.J., Downing, J.A., Cotner, J.B., Loiselle, S.A., Striegl, R.G., Ballatore, T.J., Dillon, P., Finlay, K., Fortino, K., Knoll, L.B. & Kortelainen, P.L., 2009. Lakes and reservoirs as regulators of carbon cycling and climate. *Limnology and oceanography*, *54*(6part2), pp.2298-2314.

Weishaar, J. L., Aiken, G. R., Bergamaschi, B. A., Fram, M. S., Fujii, R., & Mopper, K. (2003). Evaluation of specific ultraviolet absorbance as an indicator of the chemical composition and reactivity of dissolved organic carbon. *Environmental science & technology*, *37*(20), 4702-4708.

Zsolnay, A., Baigar, E., Jimenez, M., Steinweg, B., & Saccomandi, F. (1999). Differentiating with fluorescence spectroscopy the sources of dissolved organic matter in soils subjected to drying. *Chemosphere*, *38*(1), 45-50.

2.7 Supplemental material

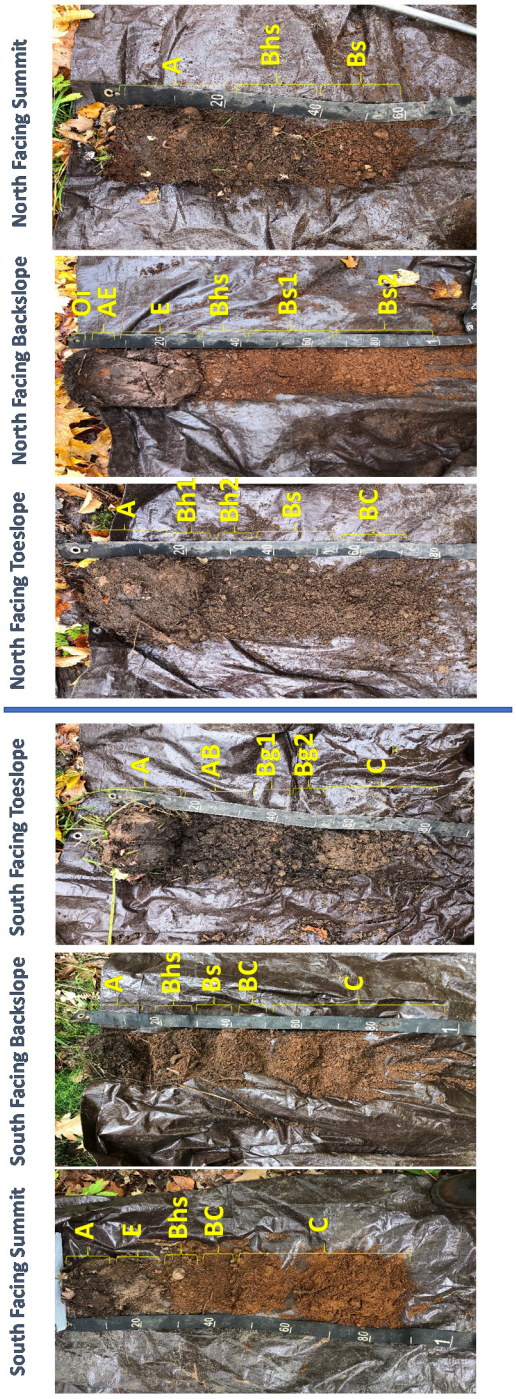

Figure S1. Images of soil profiles described in Table S1. Tape indicated profile depth is in centimeters.

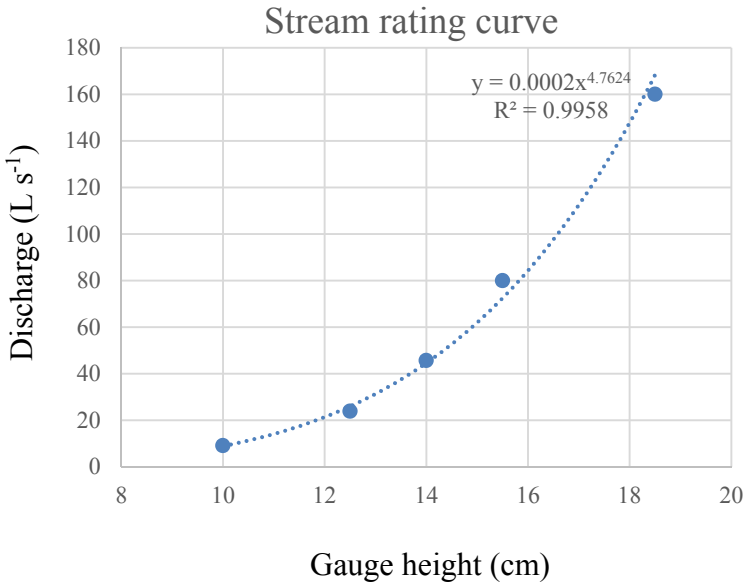

Figure S2. Stream rating curve for BGRW using the direct intercept method.

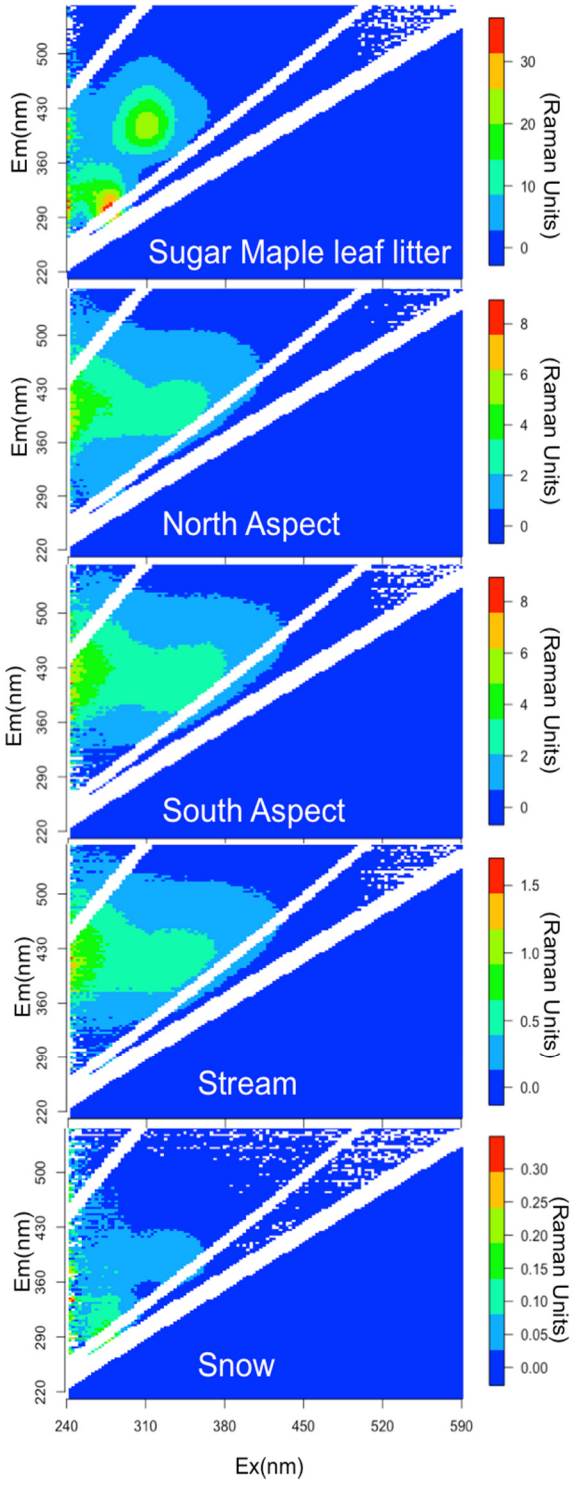
Sugar Maple leaf litter
North Aspect
South Aspect
Stream
Snow
Em(nm)
Ex(nm)
(Raman Units)

Figure S3. Representative EEMs of end members (snow and leaf litter) as well as north and south aspect soil pore water (15 cm depth) and stream runoff. Intensity is reported in Raman units.

Table S1. Soil descriptions from different slope locations for south facing and north facing aspects.

South Facing Summit

Horizonization		Boundary		Texture			Color	Structure		Consistence	Redoximorphic Features	
Master	Sub.	Lower Depth (cm)	Distinction	Sand %	Clay %	Textural Class	Hue Value/ Chroma	Grade	Shape	Moist Strength	Depletions	Concentrations
A	-	12	C	85	5	LS	10YR 2/2	2	GR	FR	-	-
E	-	18	C	88	3	LS	10YR 5/2	1	PL	VFR	-	-
B	hs	42	C	85	5	LS	7.5YR 3/4	1	SBK	VFR	-	-
BC	-	46	G	90	3	S	7.5YR 4/4	1	SBK	VFR	-	-
C	-	80+	-	91	2	S	7.5YR 4/4	0	SG	L	-	-

South Facing Backslope

Horizonization		Boundary		Texture			Color	Structure		Consistence	Redoximorphic Features	
Master	Sub.	Lower Depth (cm)	Distinction	Sand %	Clay %	Textural Class	Hue Value/ Chroma	Grade	Shape	Moist Strength	Depletions	Concentrations
A	-	19	C	80	6	SL	10YR 2/2	2	GR	FR	-	-
B	hs	30	C	85	5	LS	7.5YR 2.5/3	1	SBK	FR	-	-
B	s	41	C	85	5	LS	7.5YR 3/4	1	SBK	VFR	-	-
BC	-	52	C	88	5	LS	7.5YR 3/4	1	SBK	VFR	-	-
C	-	70+	-	92	3	S	7.5 YR 4/4	0	L	L	-	-

South Facing Toeslope

Horizonization			Boundary		Texture			Color	Structure		Consistence	Redoximorphic Features	
Master	Sub.	Note:	Lower Depth (cm)	Distinction	Sand %	Clay %	Textural Class	Hue Value/ Chroma	Grade	Shape	Moist Strength	Depletions	Concentrations
A		Mucky Mi	21	C	78	12	SL	10YR 2/1	2	SBK	FR	-	-
AB		Mucky Mi	30	C	75	12	SL	10YR 3/2	2	SBK	FR	Y	Y
B	g1		41	C	86	8	LS	10YR 3/1	2	SBK	FR	Y	Y
B	g2		52	C	86	8	LS	10YR 3/1	2	SBK	FR	Y	Y
C	g		70+	-	90	4	SL	10YR 4/2	0	SG	L	Y	Y

North Facing Toeslope

Horizonization		Boundary		Texture			Color	Structure		Consistence	Redoximorphic Features	
Master	Sub.	Lower Depth (cm)	Distinction	Sand %	Clay %	Textural Class	Hue Value/ Chroma	Grade	Shape	Moist Strength	Depletions	Concentrations
A	-	19	C	83	5	SL	7.5YR 2.5/2	2	GR	FR	-	-
B	h1	35	C	88	4	LS	7.5YR 3/3	1	SBK	FR	-	-
B	h2	40	C	88	4	LS	7.5YR 2.5/3	1	SBK	FR	-	-
B	s	57	C	86	5	LS	7.5YR 3/4	1	SBK	FR	-	-
BC		80+	-	90	3	LS	7.5YR 3/4	1	SBK	FR	-	-

North Facing Backslope

Horizonization		Boundary		Texture			Color	Structure		Consistence	Redoximorphic Features	
Master	Sub.	Lower Depth (cm)	Distinction	Sand %	Clay %	Textural Class	Hue Value/ Chroma	Grade	Shape	Moist Strength	Depletions	Concentrations
Oi	-	4	C	-	-	Fibric	10YR 2/1	-	-	-	-	-
AE	-	10	C	85	4	LS	10YR 2/3	2	PL	FR	-	-
E	-	34	G	89	4	LS	7.5YR 4/2	2	PL	FR	-	-
B	hs	41	C	86	6	LS	7.5YR 3/3	1	SBK	FR	-	-
B	s1	68	C	88	4	LS	7.5YR 3/3	1	SBK	VFR	-	-
B	s2	100+	-	89	4	LS	7.5YR 3/4	1	SBK	VFR	-	-

North Facing Summit

Horizonization		Boundary		Texture			Color	Structure		Consistence	Redoximorphic Features	
Master	Sub.	Lower Depth (cm)	Distinction	Sand %	Clay %	Textural Class	Hue Value/ Chroma	Grade	Shape	Moist Strength	Depletions	Concentrations
A	-	22	C	81	10	SL	10YR 2/2	2	GR	FR	-	-
B	hs	39	C	86	5	LS	7.5YR 3/4	1	SBK	VRF	-	-
B	s	60+	-	88	4	LS	7.5YR 4/4	1	SBK	VFR	-	-

Key

Distinction		Textural Class		Shape		Moist Strength	
C	Clear	S	Sand	SG	Single Grain	FR	Fiable
G	Gradual	LS	Loamy Sand	SBK	Subangular Blocky	VFR	Very Friable
		SL	Sandy Loam	GR	Granular	L	Loose
				PL	Platy		

3 Dissolved organic matter properties and remote sensing reflectance of river sourced plumes in Lake Superior

Karl M. Meingast[1]

Evan S. Kane[1, 2]

Colleen B. Mouw[3]

[1] Michigan Technological University; College of Forest Resources and Environmental Science; Houghton, MI

[2] U.S.D.A. Forest Service; Northern Research Station; Houghton, MI

[3] University of Rhode Island; Graduate School of Oceanography; Narragansett, RI

3.1 Abstract

Terrestrially-derived dissolved organic matter (DOM) can be a significant driver of coastal ecosystem processes. Remote sensing of freshwater coastal environments offers promise in understanding DOM inputs, hbut there are unresolved challenges associated with remotely sensed measurements of colored DOM (CDOM), particularly for smaller tributaries. This study measured DOM characteristics and reflectance spectra in a gradient from river to open lake in a region of Lake Superior with limited in-situ measurements. We found a gradient of dissolved organic carbon concentrations ranging from 17.5 mg L^{-1} in tributaries to 1.8 mg L^{-1} in coastal Lake Superior outside of direct river inputs (outside of plumes). Absorbance and fluorescence characteristics indicated a more humic and higher molecular weight DOM pool in tributaries compared to coastal Lake Superior. Reflectance spectra (convoluted Landsat OLI band specific reflectance)

were correlated with absorbance at λ=440 nm ($R^2 = 0.42$, $p = 0.02$), which was also a strong indicator of dissolved organic carbon concentrations ($R^2 = 0.87$, $p < 0.001$). These findings indicate that satellite retrievals of CDOM levels in the near-shore region of Lake Superior are highly variable, with unique reflectance properties associated with tributaries of different sizes. We demonstrate the ability of spectral surface reflectance data to detect higher levels of CDOM associated with river influence, differentiaton of CDOM levels among plumes was not possible.

3.2 Introduction

Terrestrial dissolved organic matter (DOM) strongly influences coastal ecosystem production and carbon cycling by regulating nutrient availability, light attenuation and temperature (Hopkinson et al. 1998). DOM encompasses a broad continuum of organic materials formed by the degradation of terrestrial and microbial material (Thurman et al., 1985). Changes in biogeochemical processes in soils and rivers, which are susceptible to changes induced by climate factors (Tranvik and Jansson, 2002; Roulet and Moore, 2006), can considerably alter the quantity and character of DOM as it is delivered to large lakes and coastal oceans (Peterson et al., 2002; Stedmon et al., 2011). In turn, the magnitude of DOM and mechanisms of DOM transport can alter biogeochemical processes and carbon cycling in these ecosystems (Cole et al., 2007; Tranvik et al., 2009).

Systems where a large portion of annual runoff occurs as snowmelt such as the Arctic, Sub-Arctic and Northern Great Lakes are especially vulnerable to alterations in

DOM delivery induced by climate change (Peterson et al., 2002). In these systems, winter snow accumulation, soil temperature and timing of snowmelt govern DOM transported during the spring melt. These processes are impacted by subtle changes in temperature and winter precipitation (Henry, 2008; Bjerke et al., 2015). Exactly how changes in climate are likely to affect the mechanisms of DOM delivery to aquatic environments is poorly understood (Raymond et al., 2007).

When delivered to aquatic ecosystems, the colored portion of terrestrial DOM (CDOM) has been shown to have positive feedback effects on decreases in sea ice and warming in the Arctic Sea (Pegau, 2002). Similar patterns have been observed in freshwater lakes from the Arctic to the Great Lakes (Vincent et al., 1998; Mueller et al., 2009; Arp et al., 2012; Surdu et al., 2014; Van Cleave et al., 2014). Lake Superior, largest of the Laurentian Great Lakes containing 10% of the world's freshwater, has experienced a 79% decrease in ice coverage over recent decades accompanied by increased evaporation and lower water levels (Assel et al., 2003; Wang et al., 2012). Simultaneously, warmer winters accompanied by more variation in snowfall (Hayhoe et al., 2010) have perhaps altered soil biogeochemical processes and their mechanistic linkages with terrestrial DOM pools (Stottlemyer and Toczdlowski, 1991; 1996; 2006). To date, limited *in-situ* observations leave much uncertainty in the role of terrestrially derived DOM on biological production and increasing water temperatures in Lake Superior (Bennington et al., 2012; Van Cleave et al., 2014).

Remote sensing offers a spatially-explicit tool for monitoring CDOM levels in open water. In recent studies, techniques for the remote sensing retrieval of CDOM using

spectral reflectance data have been developed specifically for Lake Superior (Shuchman et al., 2013; Binding et al., 2012; Mouw et al., 2013). However, remote sensing is limited to the detection of CDOM which is only a constituent of the total amount of dissolved organic carbon (DOC) in the water. Because the amount and quality of DOC often constrain microbial processes in aquatic ecosystems (e.g., Findlay et al., 2003), this metric is perhaps more ecologically relevant than an estimate of just the colored fraction. CDOM has been shown to directly relate to DOC in a variety of aquatic ecosystems and may hence be thought of as a tracer of DOC when a relationship between CDOM and DOC is established (Zhu and Yu, 2012). Previous research indicates that due to the relatively low amount of human activity in the Lake Superior basin (Macdonald and Minor, 2013), it is likely that DOC closely tracks CDOM in this ecosystem (Brezonik et al., 2015). However, additional research has noted seasonal and spatial variability in DOC quality relating to changes in optical properties of CDOM, most notably spectral slope of CDOM (S), in Lake Superior (Effler et al., 2010; Mouw et al., 2013). As such, additional work is needed to constrain variability in the optical properties of Lake Superior's coastal environments to refine remote sensing methods estimating CDOM levels in open water.

In this study we measured variability in near shore DOC quality, CDOM optical properties, and spectral reflectance in five tributaries of Lake Superior. Our questions focused on three issues associated with near-shore CDOM-DOC estimates:

1) What are the defining DOC characteristics of river-sourced CDOM plumes in Lake Superior, and are they different from their associated rivers?
2) Is there a constant relationship between CDOM optical properties (a_{440} nm) and DOC concentration across multiple river plumes?
3) Is there a relationship between CDOM levels and spectral reflectance data in Lake Superior river-influenced plumes?

3.3 Methods

3.3.1 Study Sites

Five river plume signatures, representative of a broad range of river sizes and flow characteristics in the Lake Superior watershed (cf. Marcarelli et al., 2019), were sampled for this study (Figure 1). The Little Elm River watershed is the smallest (40.6 km^2) and is located on the western side of the Keweenaw Peninsula. The Traverse River (65.6 km^2) discharges on the south side of the peninsula. The Elm (75.3 km^2), and the Misery (148.0 km^2) are located adjacent to the Little Elm watershed. The Ontonagon is the largest of the three watersheds (3595.6 km^2), comprising 2.6% of the Lake Superior drainage (Coble et al., 2016).

The mean annual precipitation for this region is ~ 800 mm (National Atmospheric Deposition Program; station MI99; Chassell Michigan) with over 50% of precipitation

falling as snow (Stottlemyer and Toczydlowski 2006). Mean annual temperature for the region is 4.5° C (Chapter 1).

3.3.2 Chemical and optical analyses

Samples and reflectance analyses were collected from each of the study sites from a 4m inflatable boat navigating from within the river, to the plume center (determined *a priori* with remote sensing imagery and geographic positioning system), and then outside of the plume at each watershed. Samples were immediately filtered with 0.45 μm PVDF syringe filters into opaque HDPE containers and transported in a cooler back to Michigan Tech for analysis.

Absorption and fluorescence spectra were analyzed using a Horiba Aqualog fluorometer (Horiba–Jobin–Yvon Aqualog C; Horiba Co., Edison, NJ) in 1 cm quartz cells (Starna Cells, Inc). Absorption spectra were run from 240 nm to 600 nm at 3 nm resolution. Fluorescence spectra were recorded at 3 nm excitation wavelengths from 240 nm to 600 nm and emission was recorded at 3 nm resolution from 240 nm to 640 nm (Figure S3). Fluorescence spectra were converted to Raman units (R.U.) using Raman scattering from a sealed Milli-Q cuvette (Starna) (R.U.) (Lawaetz and Stedmon, 2009). Absorbance values were converted to Naperian absorption coefficients (a_λ) (Green and Blough, 1994):

$$a_\lambda = 2.303 \frac{A_\lambda}{L} \quad (1)$$

Where A_λ is absorbance at wavelength λ, and L is the path-length, in meters. Inner filter effects, Raman scattering, and Raleigh scattering for fluorescence EEMs were corrected for inner filter effects using the flucut function in PLS toolbox (version 782; Eigenvector) in Matlab (r2014a). We derived two specific spectral slopes ($S_{275\text{-}295}$ and $S_{350\text{-}400}$) from the absorption spectra as indicators of average DOM molecular weight (Helms et al., 2008), and these were calculated as the slopes of the linear regressions of log-transformed absorption spectra from 275-295 nm and 350-400 nm, respectively.

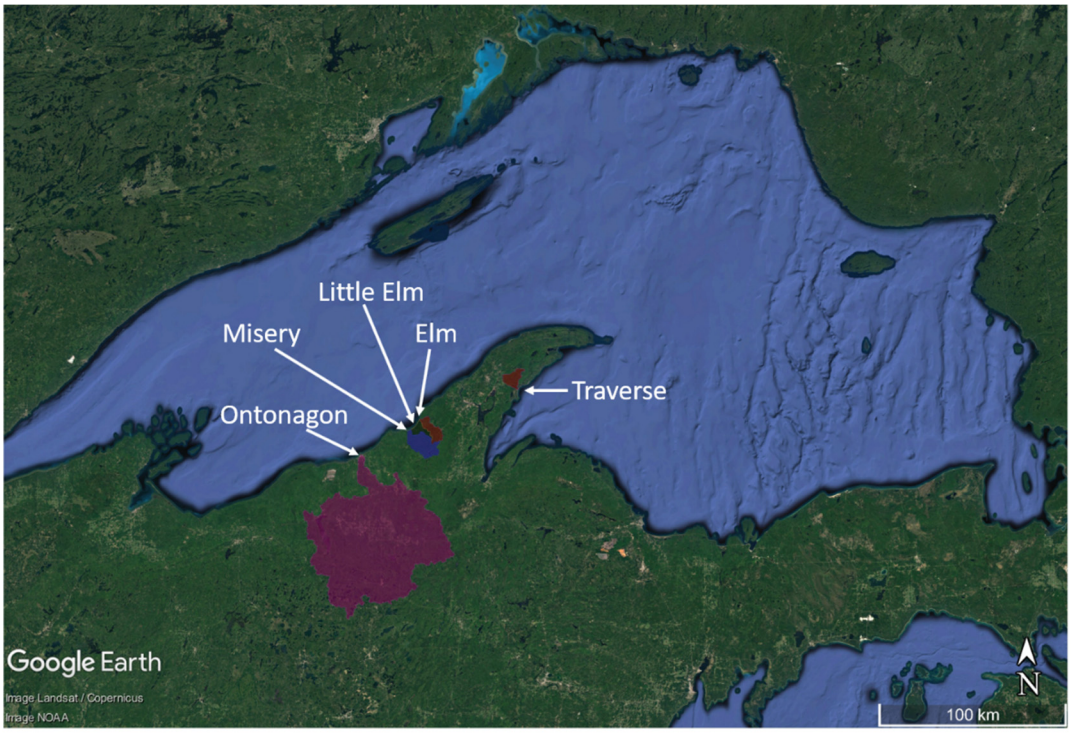

Figure 1: The five river watersheds sampled in this study from across the Keweenaw Peninsula of Michigan. Colored regions denote watershed areas.

From the fluorescence spectra measurements, we calculated three parameters. The biological index (BIX), used to differentiate terrestrial reference standards from phytoplankton derived DOM (Osburn et al., 2019) and humification index (HIX), an index of soil humification (Zolsnay et al., *1999;* Ohno, 2002) and were defined as:

$$BIX = \frac{F_{380}}{F_{430}} \quad (2)$$

Where F_{380} and F_{430} are the fluorescence emission intensities at 380 and 430 nm, respectively at excitation 310 nm.

$$HIX = \frac{\Sigma F_{435-480}}{\Sigma F_{300-345}} \quad (3)$$

Where $\Sigma F_{435-480}$ is the sum of the fluorescence emission from 435 to 480 nm and $\Sigma F_{300-345}$ is the sum of the fluorescence emission from 300 – 345 nm at excitation of 254 nm.

The ratio of fluorescence Peak C to Peak A (C/A), which has been shown to inversely track photodegradation of *DOM* (Coble, 1996; Hansen et al. 2016) as well as the degree of humic substance degradation or oxidation (Moran et al. 2000; Kothawala et al. 2012) was calculated as:

$$C/A = \frac{F_{ex340/em440}}{F_{ex260/em450}} \quad (4)$$

Where $F_{ex340/em440}$ is fluorescence intensity at excitation 340 nm and emission wavelength 440 nm. $F_{ex260/em450}$ is fluorescence intensity at excitation 260 nm and emission wavelength 450 nm. All samples were acidified to pH 2 with HCl (VWR) and analyzed for total organic carbon with a Shimadzu TOC-V analyzer (Shimadzu; Kyoto, Japan). We report the specific absorbance normalized by DOC concentration of the sample ($SUVA_{254}$) as a metric to quantify the amount of chromophoric DOM in the sample, which has also been related to DOM aromaticity (Weishaar et al. 2003). We also report absorption at 440 nm (a_{440}) which has been used as a proxy for CDOM levels in complex waters (Brezonik et al. 2015). Secchi depth was also recorded when depth to bottom was sufficient.

3.3.3 Radiometry

Remotely sensed reflectance (R_{rs}) measurements were measured using two methods. (1) Sequential measurements were made of water surface and normalized to plaque radiances using a white reference panel (Spectralon). Three scans were collected and the mean was used for analysis. For these measurements we employed an ASD Fieldspec 3 spectroradiometer (Analytical Spectral Devices, Boulder, CO). (2) We measured upwelling radiance directly below the water surface using a 20° foreoptic (ASD) and normalizing to sky irradiance as measured with a Remote Cosine Receptor (ASD). Three scans were collected and the mean was used for analysis. Because of the lack of relationship between these two measurements, this study employs the sequential

measurement technique. The average of three scans is reported. Reflectance spectra were convoluted to the relative spectral response curves of Landsat 8 Operational Land Imager (OLI) bands by multiplying reflectance spectra by the relative response of each band by wavelength (cf. Meingast et al. 2014). Spectral response curves were acquired from (https://landsat.usgs.gov/spectral-characteristics-viewer).

3.3.4 Statistics

Relationships among a_{440} and DOC, and $R_{rs\ to}\ a_{440}$ were determined using linear regressions in R (R Core Team 2014). A one-way analysis of variance (ANOVA) with a Tukey's honest significant difference (HSD) test was used to assess mean differences in absorption and fluorescence indices among sampling locations.

Table 1: Optical characteristics of river, plume and Lake Superior DOM

	Date	Lat/Long	a440 (m^{-1})	S275-295	S350-400	C/A	HIX	BIX	DOC (mg L^{-1})	SUVA 254 (L mg C^{-1} m^{-1})	Secchi depth (m)
Elm and Little Elm Rivers out of plume	5-May-16	47.0372/-88.9327	0.28	0.019	0.020	0.46	4.1	0.56	3.1	1.3	7.5
Elm River plume	5-May-16	47.0462/-88.9224	0.33	0.017	0.021	0.53	7.6	0.53	4.1	1.6	On bottom
Little Elm River Plume	5-May-16	47.0363/-88.9292	0.88	0.017	0.019	0.53	7.8	0.58	3.8	2.8	On bottom
Elm River	5-May-16	--	3.97	0.013	0.016	0.67	21.3	0.48	7.3	3.7	--
Little Elm River	5-May-16	--	4.39	0.015	0.018	0.75	28.4	0.48	10.6	3.6	--
Traverse River out of plume	3-Jun-16	47.1873/-88.2335	0.30	0.021	0.015	0.52	3.9	0.62	3.2	1.1	5.5
Traverse River plume	3-Jun-16	47.1877/-88.2351	5.22	0.014	0.017	0.71	24.5	0.46	9.4	3.9	4
Traverse River	3-Jun-16	47.1909/-88.2367	12.12	0.013	0.017	0.85	41.7	0.43	17.5	4.9	--
Misery River out of plume	17-Jun-16	47.0020/-88.9851	0.25	0.023	0.017	0.43	3.1	0.76	3.5	1.1	On bottom
Misery Plume	17-Jun-16	47.0007/-88.9787	2.36	0.015	0.017	0.58	14.3	0.54	6.3	2.9	On bottom
Misery river	17-Jun-16	--	3.49	0.015	0.017	0.63	18.6	0.53	7.6	3.4	--
Ontonagon River out of plume	7-Jun-17	46.8789/-89.3328	1.64	0.017	0.011	1.03	2.5	0.61	3.5	2	--
Ontonagon Plume	7-Jun-17	46.8804/-89.3298	8.16	0.014	0.014	0.68	17.7	0.49	8.4	4.7	--
Ontonagon River	7-Jun-17	46.8736/-89.3245	8.17	0.014	0.015	0.67	17.1	0.46	10.7	4.4	--
Ontonagon River out of plume	8-Jun-18	46.8774/-89.3545	0.29	0.018	0.015	0.19	0.6	2.32	1.8	2	8.5
Ontonagon Plume	8-Jun-18	46.8814/-89.3310	4.62	0.014	0.016	0.62	10.9	0.57	6.0	5.3	1
Ontonagon River	8-Jun-18	46.8740/-89.3238	7.66	0.014	0.016	0.72	22.6	0.49	11.2	4.6	--
Ontonagon River	30-Aug-18	46.8737/-89.3244	3.51	0.016	0.017	0.63	11.2	0.61	--	--	--
Ontonagon Plume	30-Aug-18	46.8824/-89.3291	2.65	0.016	0.017	0.58	5.6	0.77	--	--	--
Ontonagon River out of plume	30-Aug-18	46.8824/-89.3451	0.50	0.024	0.013	0.61	1.2	1.42	--	--	--

Table 2: Absorption and fluorescence indices (mean and standard error) from tributaries, plumes and open lake stations. Letters indicate significant differences among locations. Ontonagon samples collect 30-Aug-2018 were not included due to missing data.

	a440 (m^{-1})	S275-295	S350-400	C/A	HIX	BIX	DOC ($mg\ L^{-1}$)	$SUVA_{254}$ ($L\ mg\ C^{-1}\ m^{-1}$)
Rivers	6.64(0.95)[a]	0.014(0.002)[a]	0.017(0.002)[a]	0.71(0.14)[a]	24.9(4.4)[a]	0.5(0.4)[a]	10.8(1.3)[a]	4.1(0.5)[a]
Plumes	3.60(0.96)[a,b]	0.015(0.002)[a]	0.017(0.001)[a]	0.61(0.14)[a]	13.8(4.4)[b]	0.5(0.4)[b]	6.3(1.3)[b]	3.5(0.5)[a]
Lake	0.55(0.27)[b]	0.020(0.001)[b]	0.016(0.001)[a]	0.52(0.14)[a]	2.8(0.6)[c]	1.0(0.3)[c]	3.0(0.3)[b]	1.5(0.2)[b]

3.4 Results

3.4.1 CDOM characteristics

$S_{275-295}$ ranged from 0.013 to 0.023 nm^{-1} with the lowest values exhibited in tributaries (Table 2). $S_{350-400}$ ranged from 0.011 to 0.020, and were less variable across sampling positions than $S_{275-295}$ (Table 2). HIX ranged from 0.6 outside of plumes in Lake Superior to 41.7 in the Traverse River (Table 1). HIX and BIX were the only metrics to show significant differences among all three locations (Table 2). BIX ranged from 0.43 to 2.32. The maximum was recorded in Lake Superior outside of plumes and the minimum was collected in the Traverse River. HIX and BIX were strongly negatively correlated (Figure 2). C/A ranged from 0.18 to 1.02 with both the minimum and maximum recorded outside of plumes. SUVA ranged from 1.1 to 5.3 L mg C^{-1} m^{-1} and was generally lowest

outside of river plumes.

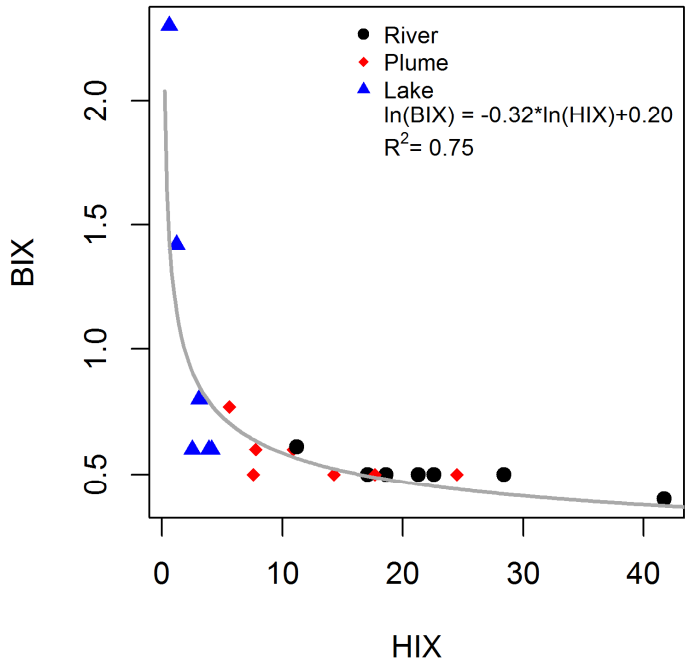

Figure 2: Plot of HIX vs BIX for this study.

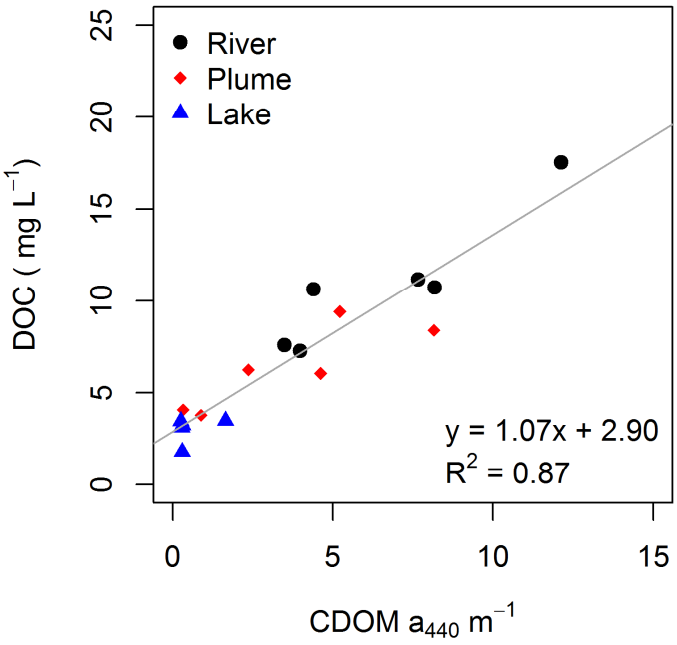

Figure 3: a_{440} vs DOC relationship in this study (n = 16).

3.4.2 CDOM and DOC relationship

DOC ranged from 1.8 to 17.5 mg L^{-1} in this study. Rivers had the highest values and ranged from 3.1 to 17.5 mg L^{-1} DOC. Plumes had intermediate values and ranged from 3.8 to 9.4 mg L^{-1}. Lake Superior outside of plumes only ranged from 1.8 to 3.5 mg L^{-1}. CDOM a_{440} ranged from 0.25 to 12.12 m^{-1} in the study. Rivers ranged from 3.97 to 12.12 m^{-1}. Plumes ranged from 0.33 to 8.16 m^{-1}. Lake Superior outside of plumes ranged from 0.28 to 1.64 m^{-1}. There was a strong linear relationship between CDOM a_{440} and DOC (Figure 3) with a regression line slope of 1.07 (S.E. = 0.10) mg m L^{-1}.

3.4.3 Reflectance spectra characteristics and relationship to a_{440}

Reflectance spectra in river plumes were similar excluding the Ontonagon Plume which exhibited much higher R_{rs}, primarily from 550 to 700 nm (Figure 4). When convoluted to Landsat OLI band specific reflectance, the natural log of the ratio of Landsat OLI Band 3 (530 – 590 nm) to Band 4 (640 – 670 nm) was linearly correlated with the natural log of CDOM a_{440} ($R^2 = 0.42$; $p = 0.02$; Figure 5). When R_{rs} was calculated as the ratio of upwelling radiance below the water surface divided by downwelling solar irradiance, the ratio of Landsat 8 Band 3/Band4 was not correlated with the above surface reflectance or CDOM a_{440} (data not shown).

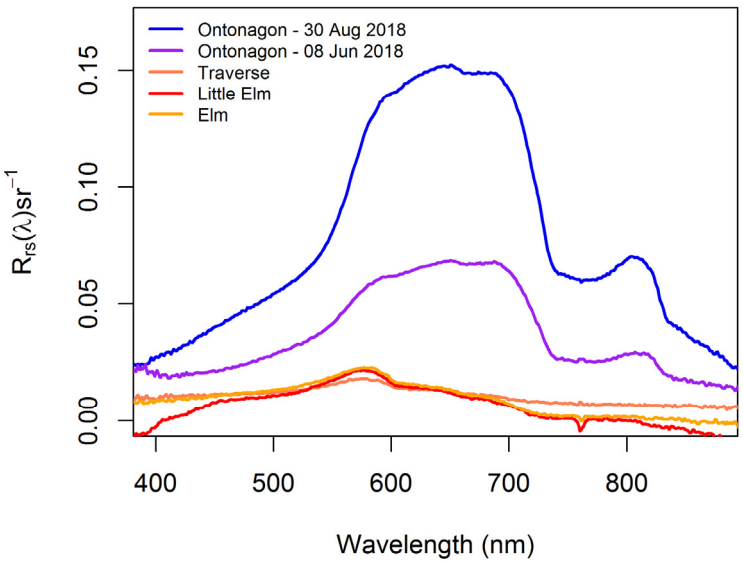

Figure 4: Representative reflectance spectra for the study river plumes. The Misery River reflectance spectra were not valid and therefore were not used in the analysis, however absorbance, fluorescence and DOC data were used to develop empirical relationships.

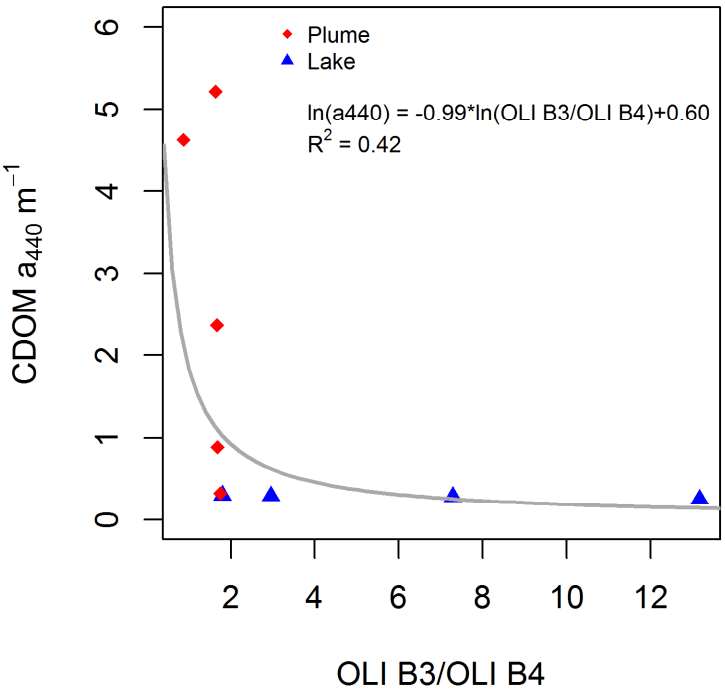

Figure 5: Relationship between Landsat OLI Band 3 / Landsat OLI B4 and CDOM levels at plume and out of plume (Lake) stations.

3.5 Discussion

3.5.1 CDOM characteristics

$S_{275-295}$ is lowest in the tributaries (Table 1), indicating that average molecular weight was highest in tributaries (Helms et al. 2008). This finding suggests that terrestrially derived, high molecular weight DOM influences oceanic waters (Stedmon and Markager, 2001; Stedmon et al., 2011). Loss of larger molecular weight DOM was expected in the Ontonagon and Misery rivers due to preferential adsorption of higher molecular weight DOM to sediment particles (Osburn et al., 2009). However, our results indicate slightly lower $S_{275-295}$ and $S_{350-400}$ in the Ontonagon and Misery with visibly higher sediment loads. Preferential adsorption and limited photo-degradation by suspended sediment provide parsimonious mechanisms for the lower slope values in the high sediment load tributaries.

HIX values ranged from 7.6 to 41.7 in all rivers and plumes, indicating a strongly humified DOM pool at all station within this study (Huguet et al., 2009). These results suggest that this humic material was likely of allochthonous origin to the lake, likely derived from soil processing (Chapter 2), and was largely recalcitrant when delivered to Lake Superior. However, the lower HIX values reported here have also been reported at more offshore regions of Lake Superior (Marcarelli et al., 2019), indicating that these materials are not impervious to degradation in Lake Superior. $SUVA_{254}$ also trended with HIX indicating a general decrease in aromaticity from rivers to lake. The associated low

BIX values are also indicative of DOM that is not of autochthonous origin and are likely terrestrially derived (Huguet et al., 2009; Figure 2). One interesting exception is the June 8, 2018 sample outside of the Ontonagon River plume, which exhibited a BIX of 2.3, over four times greater than the mean value for this study. Results from Huguet et al. (2009) suggest that this sample is likely of autochthonous origin, potentially the only sample in this study with these characteristics.

3.5.2 CDOM and DOC relationship

Remote sensing studies measuring CDOM often assume that CDOM levels can be converted into DOC concentrations (Kutser et al., 2005; Brezonik et al., 2015). Absorption coefficients between 400-450 nm are often used as proxies for CDOM levels because they fall within the range of satellite sensor detection (Brezonik et al., 2015). The relationship between a_{440} as an indicator of CDOM and DOC was quite strong ($R^2 = 0.87$; Figure 3) indicating that CDOM levels (specifically a_{440}) can be used in this region as an indicator of DOC concentration. However, these relationships are often not constant (Worrall & Burt, 2010) and must be interpreted with caution. Furthermore, this relationship does not indicate zero DOC is associated with zero CDOM, indicating that this relationship is not linear at lower DOC concentrations or that the intercept is not zero and is likely most applicable in river-influenced regions of Lake Superior.

3.5.3 Reflectance spectra characteristics and relationship to a_{440}

The general shape of river plume reflectance spectra varied substantially between plumes (Figure 4). Most notably, the reflectance spectra of the Ontonagon had a maximum R_{rs} ranging between 0.05 and 0.15 sr^{-1}. These values are generally indicative of turbid waters (Kutser et al., 2001). The Traverse, Little Elm, and Elm appeared similar, with much lower R_{rs} and a maximum reflectance between 550 – 600 nm. This is likely a signature of CDOM dominated tributaries and is a defining characteristic of these river plumes.

When convoluted to band specific responses for Landsat 8, the ratio of Band 3 to Band 4 showed the only significant relationship with CDOM ($R^2 = 0.42$; $p = 0.02$; Figure 5), which is in line with previous studies nominating this ratio as the strongest indicator of CDOM levels (Kurtser et al., 2005; Brezonik et al., 2015). However, quasi-analytical algorithms (QAAs) have been developed in Lake Superior using the Moderate Resolution Imaging Spectroradiometer (MODIS) to more accurately quantify CDOM levels (Mouw et al., 2013). Although this sensor likely lacks adequate spatial resolution for application in coastal systems, recent advances in applications of these QAAs to Landsat imagery (Wei et al., 2019) may provide a tool for increasing the accuracy and constraining error estimates for CDOM levels in Lake Superior. Future work is necessary to assess the utility and adjust quasi-analytical algorithms for use in complex Lake Superior waters.

3.6 Conclusions

This study sampled five rivers for DOC quality and concentration as well as spectral reflectance associated with each. We found DOC to be generally humic-like as

indicated by HIX and of various average molecular weights as indicated by spectral slopes. $SUVA_{254}$ was also highly variable indicating various degrees of aromaticity throughout the study rivers. DOC concentrations were moderate and variable, with rivers discharging the highest DOC concentrations. Spectral properties and DOC concentrations varied across tributaries, and unique DOM characteristics of rivers were reflected in the plumes into Lake Superior.

A significant relationship was evident between spectral response curves and CDOM levels (a_{440}). This relationship, although significant, displays the variable nature of DOM in this region and therefore indicates that satellite retrievals in the near-shore region of CDOM levels are likely accompanied by relatively high levels of uncertainty. Therefore, we recommend specific relationships be developed for CDOM levels in individual river plumes for Lake Superior for highest accuracy between rivers. However, the work presented here demonstates the ability for remote sensing platforms to differentiate plume signatures from open lake signatures. Building on the work presented here, specifically for the relatively large Ontonagon River, would aid in the utility of satellite sensors to monitor DOC loadings to Lake Superior.

3.7 References

Arp, C.D., Jones, B.M., Lu, Z. and Whitman, M.S., 2012. Shifting balance of thermokarst lake ice regimes across the Arctic Coastal Plain of northern Alaska. *Geophysical Research Letters*, *39*(16).

Assel, R., Cronk, K. and Norton, D., 2003. Recent trends in Laurentian Great Lakes ice cover. *Climatic Change*, *57*(1-2), pp.185-204.

Bennington, V., McKinley, G.A., Urban, N.R. and McDonald, C.P., 2012. Can spatial heterogeneity explain the perceived imbalance in Lake Superior's carbon budget? A model study. *Journal of Geophysical Research: Biogeosciences*, *117*(G3).

Binding, C. E., Greenberg, T. A., & Bukata, R. P., 2012. An analysis of MODIS-derived algal and mineral turbidity in Lake Erie. *Journal of Great Lakes Research*, *38*(1), 107–116. doi:10.1016/j.jglr.2011.12.003

Bjerke, J.W., Tømmervik, H., Zielke, M. and Jørgensen, M., 2015. Impacts of snow season on ground-ice accumulation, soil frost and primary productivity in a grassland of sub-Arctic Norway. *Environmental Research Letters*, *10*(9), p.095007.

Brezonik, P.L., Olmanson, L.G., Finlay, J.C. and Bauer, M.E., 2015. Factors affecting the measurement of CDOM by remote sensing of optically complex inland waters. *Remote Sensing of Environment*, *157*, pp.199-215.

Coble, P.G., 1996. Characterization of marine and terrestrial DOM in seawater using excitation-emission matrix spectroscopy. *Marine chemistry*, *51*(4), pp.325-346.

Coble, A.A., Marcarelli, A.M., Kane, E.S. and Huckins, C.J., 2016. Uptake of ammonium and soluble reactive phosphorus in forested rivers: influence of dissolved organic matter composition. *Biogeochemistry*, *131*(3), pp.355-372.

Cole, J.J., Prairie, Y.T., Caraco, N.F., McDowell, W.H., Tranvik, L.J., Striegl, R.G., Duarte, C.M., Kortelainen, P., Downing, J.A., Middelburg, J.J. and Melack, J., 2007. Plumbing the global carbon cycle: integrating inland waters into the terrestrial carbon budget. *Ecosystems*, *10*(1), pp.172-185.

Effler, S.W., Perkins, M., Peng, F., Strait, C., Weidemann, A.D., Auer, M.T., 2010. Light-absorbing components in Lake Superior. J. Great Lakes Res. 36, 656–665. doi:10.1016/j.jglr.2010.08.001

Evans, C.D., Monteith, D.T. and Cooper, D.M., 2005. Long-term increases in surface water dissolved organic carbon: observations, possible causes and environmental impacts. *Environmental pollution*, *137*(1), pp.55-71.

Findlay S., 2003. Bacterial response to variation in dissolved organic matter. Aquatic Ecosystems: Interactivity of Dissolved Organic Matter; edited by: Findlay, S.E.G., Sinsabaugh, R.L.; Academic Press. pp. 363-382.

Green, S.A. and Blough, N.V., 1994. Optical absorption and fluorescence properties of chromophoric dissolved organic matter in natural waters. *Limnology and Oceanography*, *39*(8), pp.1903-1916.

Hansen, A.M., Kraus, T.E., Pellerin, B.A., Fleck, J.A., Downing, B.D. and Bergamaschi, B.A., 2016. Optical properties of dissolved organic matter (DOM): Effects of biological and photolytic degradation. *Limnology and Oceanography*, *61*(3), pp.1015-1032.

Hayhoe, K., VanDorn, J., Croley II, T., Schlegal, N. and Wuebbles, D., 2010. Regional climate change projections for Chicago and the US Great Lakes. *Journal of Great Lakes Research*, *36*, pp.7-21.

Helms, J.R., Stubbins, A., Ritchie, J.D., Minor, E.C., Kieber, D.J. and Mopper, K., 2008. Absorption spectral slopes and slope ratios as indicators of molecular weight, source, and photobleaching of chromophoric dissolved organic matter. *Limnology and Oceanography*, *53*(3), pp.955-969.

Henry, H.A., 2008. Climate change and soil freezing dynamics: historical trends and projected changes. *Climatic Change*, *87*(3-4), pp.421-434.

Hopkinson, C.S., Buffam, I., Hobbie, J., Vallino, J., Perdue, M., Eversmeyer, B., Prahl, F., Covert, J., Hodson, R., Moran, M.A. and Smith, E., 1998. Terrestrial inputs of organic matter to coastal ecosystems: an intercomparison of chemical characteristics and bioavailability. *Biogeochemistry*, *43*(3), pp.211-234.

Huguet, A., Vacher, L., Relexans, S., Saubusse, S., Froidefond, J.M. and Parlanti, E., 2009. Properties of fluorescent dissolved organic matter in the Gironde Estuary. *Organic Geochemistry*, *40*(6), pp.706-719.

Kothawala, D.N., von Wachenfeldt, E., Koehler, B. and Tranvik, L.J., 2012. Selective loss and preservation of lake water dissolved organic matter fluorescence during long-term dark incubations. *Science of the Total Environment*, *433*, pp.238-246.

Kutser, T., Herlevi, A., Kallio, K. and Arst, H., 2001. A hyperspectral model for interpretation of passive optical remote sensing data from turbid lakes. *Science of the Total Environment*, *268*(1-3), pp.47-58.

Kutser, T., Pierson, D.C., Kallio, K.Y., Reinart, A. and Sobek, S., 2005. Mapping lake CDOM by satellite remote sensing. *Remote Sensing of Environment*, *94*(4), pp.535-540.

Lawaetz, A.J. and Stedmon, C.A., 2009. Fluorescence intensity calibration using the Raman scatter peak of water. *Applied spectroscopy*, *63*(8), pp.936-940.

Macdonald, M.J. and Minor, E.C., 2013. Photochemical degradation of dissolved organic matter from rivers in the western Lake Superior watershed. *Aquatic sciences*, *75*(4), pp.509-522.

Marcarelli, A.M., Coble, A.A., Meingast, K.M., Kane, E.S., Brooks, C.N., Buffam, I., Green, S.A., Huckins, C.J., Toczydlowski, D. and Stottlemyer, R., 2019. Of small rivers and Great Lakes: integrating tributaries to understand the ecology and biogeochemistry of Lake Superior. *JAWRA Journal of the American Water Resources Association*, *55*(2), pp.442-458.

Meingast, K.M., Falkowski, M.J., Kane, E.S., Potvin, L.R., Benscoter, B.W., Smith, A.M., Bourgeau-Chavez, L.L. and Miller, M.E., 2014. Spectral detection of near-surface moisture content and water-table position in northern peatland ecosystems. *Remote sensing of environment*, *152*, pp.536-546.

Moran, M.A., Sheldon Jr, W.M. and Zepp, R.G., 2000. Carbon loss and optical property changes during long-term photochemical and biological degradation of estuarine dissolved organic matter. *Limnology and Oceanography*, *45*(6), pp.1254-1264.

Mouw, C. B., Chen, H., McKinley, G. A., Effler, S., O'Donnell, D., Perkins, M. G., et al., 2013.Evaluation and optimization of bio-optical inversion algorithms for remote sensing of Lake Superior's optical properties. *Journal of Geophysical Research*, 118, 1696–1714, http://dx.doi.org/10.1002/jgrc.20139.

Mouw, C.B., Greb, S., Aurin, D., DiGiacomo, P.M., Lee, Z., Twardowski, M., Binding, C., Hu, C., Ma, R., Moore, T. and Moses, W., 2015. Aquatic color radiometry remote sensing of coastal and inland waters: Challenges and recommendations for future satellite missions. *Remote sensing of environment*, *160*, pp.15-30.

Mueller, D.R., Van Hove, P., Antoniades, D., Jeffries, M.O. and Vincent, W.F., 2009. High Arctic lakes as sentinel ecosystems: Cascading regime shifts in climate, ice cover, and mixing. *Limnology and Oceanography*, *54*(6part2), pp.2371-2385.

Ohno, T., 2002. Fluorescence inner-filtering correction for determining the humification index of dissolved organic matter. *Environmental science & technology*, *36*(4), pp.742-746.

Osburn, C.L., Retamal, L. and Vincent, W.F., 2009. Photoreactivity of chromophoric dissolved organic matter transported by the Mackenzie River to the Beaufort Sea. *Marine Chemistry*, *115*(1-2), pp.10-20.

Osburn, C.L., Kinsey, J.D., Bianchi, T.S. and Shields, M.R., 2019. Formation of planktonic chromophoric dissolved organic matter in the ocean. *Marine Chemistry*, *209*, pp.1-13.

Pegau, W. S., 2002. Inherent optical properties of the central Arctic surface waters, J. Geophys. Res., 107(C10), 8035, doi:10.1029/2000JC000382.

Peterson, B.J., Holmes, R.M., McClelland, J.W., Vörösmarty, C.J., Lammers, R.B., Shiklomanov, A.I., Shiklomanov, I.A. and Rahmstorf, S., 2002. Increasing river discharge to the Arctic Ocean. *science*, *298*(5601), pp.2171-2173.

R Core Team (2014). R: A language and environment for statistical computing. R Foundation for Statistical Computing, Vienna, Austria. URL http://www.R-project.org/.

Raymond, P.A., McClelland, J.W., Holmes, R.M., Zhulidov, A.V., Mull, K., Peterson, B.J., Striegl, R.G., Aiken, G.R. and Gurtovaya, T.Y., 2007. Flux and age of dissolved organic carbon exported to the Arctic Ocean: A carbon isotopic study of the five largest arctic rivers. *Global Biogeochemical Cycles*, *21*(4).

Roulet, N. and Moore, T.R., 2006. Browning the waters. *Nature*, *444*(7117), pp.283-284.

Shuchman, R.A., Leshkevich, G., Sayers, M.J., Johengen, T.H., Brooks, C.N. and Pozdnyakov, D., 2013. An algorithm to retrieve chlorophyll, dissolved organic carbon, and suspended minerals from Great Lakes satellite data. *Journal of Great Lakes Research*, *39*, pp.14-33.

Stedmon, C.A. and Markager, S., 2001. The optics of chromophoric dissolved organic matter (CDOM) in the Greenland Sea: An algorithm for differentiation between marine and terrestrially derived organic matter. *Limnology and Oceanography*, *46*(8), pp.2087-2093.

Stedmon, C.A., Amon, R.M.W., Rinehart, A.J. and Walker, S.A., 2011. The supply and characteristics of colored dissolved organic matter (CDOM) in the Arctic Ocean: Pan Arctic trends and differences. *Marine Chemistry*, *124*(1-4), pp.108-118.

Stottlemyer, R. and Toczydlowski, D., 1991. Stream chemistry and hydrologic pathways during snowmelt in a small watershed adjacent Lake Superior. *Biogeochemistry*, *13*(3), pp.177-197.

Stottlemyer, R. and Toczydlowski, D., 1996. Modification of snowmelt chemistry by forest floor and mineral soil, Northern Michigan. *Journal of environmental quality*, *25*(4), pp.828-836.

Stottlemyer, R. and Toczydlowski, D., 2006. Effect of reduced winter precipitation and increased temperature on watershed solute flux, 1988–2002, Northern Michigan. *Biogeochemistry*, *77*(3), pp.409-440.

Surdu, C.M., Duguay, C.R., Brown, L.C. and Prieto, D.F., 2014. Response of ice cover on shallow lakes of the North Slope of Alaska to contemporary climate conditions (1950-2011): Radar remote-sensing and numerical modeling data analysis. *The Cryosphere*, *8*(1), p.167.

Thurman, E.M., 1985. Amount of organic carbon in natural waters. In *Organic geochemistry of natural waters* (pp. 7-65). Springer, Dordrecht.

Tranvik, L.J. and Jansson, M., 2002. Terrestrial export of organic carbon. *Nature*, *415*(6874), pp.861-862.

Tranvik, L.J., Downing, J.A., Cotner, J.B., Loiselle, S.A., Striegl, R.G., Ballatore, T.J., Dillon, P., Finlay, K., Fortino, K., Knoll, L.B. and Kortelainen, P.L., 2009. Lakes and reservoirs as regulators of carbon cycling and climate. *Limnology and oceanography*, *54*(6part2), pp.2298-2314..

Van Cleave, K., Lenters, J.D., Wang, J. and Verhamme, E.M., 2014. A regime shift in Lake Superior ice cover, evaporation, and water temperature following the warm El Niñ winter of 1997–1998. *Limnology and Oceanography*, *59*(6), pp.1889-1898.

Vincent, W.F., Rae, R., Laurion, I., Howard-Williams, C. and Priscu, J.C., 1998. Transparency of Antarctic ice-covered lakes to solar UV radiation. *Limnology and oceanography*, *43*(4), pp.618-624.

Wang, J., Bai, X., Hu, H., Clites, A., Colton, M. and Lofgren, B., 2012. Temporal and spatial variability of Great Lakes ice cover, 1973–2010. *Journal of Climate*, *25*(4), pp.1318-1329.

Wei, J., Lee, Z., Shang, S. and Yu, X., 2019. Semianalytical derivation of phytoplankton, CDOM, and detritus absorption coefficients from the Landsat 8/OLI reflectance in coastal waters. *Journal of Geophysical Research: Oceans*, *124*(6), pp.3682-3699.

Weishaar, J.L., Aiken, G.R., Bergamaschi, B.A., Fram, M.S., Fujii, R. and Mopper, K., 2003. Evaluation of specific ultraviolet absorbance as an indicator of the chemical

composition and reactivity of dissolved organic carbon. *Environmental science & technology*, *37*(20), pp.4702-4708.

Worrall, F. and Burt, T.P., 2010. Has the composition of fluvial DOC changed? Spatiotemporal patterns in the DOC-color relationship. *Global Biogeochemical Cycles*, *24*(1).

Zhu, W. and Yu, Q., 2012. Inversion of chromophoric dissolved organic matter from EO-1 Hyperion imagery for turbid estuarine and coastal waters. *IEEE Transactions on Geoscience and Remote Sensing*, *51*(6), pp.3286-3298.

Zsolnay, A., Baigar, E., Jimenez, M., Steinweg, B. and Saccomandi, F., 1999. Differentiating with fluorescence spectroscopy the sources of dissolved organic matter in soils subjected to drying. *Chemosphere*, *38*(1), pp.45-50.